Title: Environmental impacts on walleye pollock (*Gadus chalcogrammus*) distribution across the Bering Sea shelf

Authors: Lisa B. Eisner[a*], Yury Zuenko[b], Eugene Basyuk[b], Lyle Britt[a], Janet T. Duffy-Anderson[a], Stan Kotwicki[a], Carol Ladd[c], Wei Cheng[c,d]

*corresponding author

[a] NOAA Alaska Fisheries Science Center, Seattle WA, USA; lisa.eisner@noaa.gov; lyle.britt@noaa.gov; janet.duffy-anderson@noaa.gov; stan.kotwicki@noaa.gov

[b] Russian Research Institute of Fisheries and Oceanography, Pacific Branch (TINRO), Vladivostok, RUSSIA; zuenko_yury@hotmail.com; evgeniy.basyuk@tinro-center.ru

[c] NOAA Pacific Marine Environmental Lab, Seattle WA, USA; carol.ladd@gmail.com

[d] University of Washington, Cooperative Institute for Climate, Ocean and Ecosystem Studies, Seattle, WA, USA; wei.cheng@noaa.gov

ABSTRACT

Adult and juvenile (age-1) walleye pollock (*Gadus chalcogrammus*) were sampled by the US NOAA Alaska Fisheries Science Center summer bottom trawl survey in 2010, 2017, 2018, and 2019 in the northeastern and southeastern Bering Sea, with profiles of temperature collected concurrently. Similarly, the Russian Research Institute of Fisheries and Oceanography, Pacific branch, collected adult and juvenile pollock and temperature profiles on summer bottom trawl surveys in the northwestern Bering Sea. Results from these surveys show that adult pollock abundance in recent years (2017, 2018, 2019) has increased in northern regions of the Bering Sea shelf in both the US and Russian sectors. Lower abundances, compared to historic means, were observed in southern regions of the shelf, suggesting the pollock moved directionally from the south to the north. We relate changes in pollock distribution in recent intermediate (2017) and warm, low-ice years (2018–2019) to a prior cold, high-ice year (2010) and describe how these observations relate to our longer time series. We link temperature data from bottom trawl surveys (US and Russian), sea-ice indices (retreat timing and extent), as well as model-based estimates of ocean circulation to changes in pollock distribution and examine potential environmental factors driving the observed changes. Changes in sea-ice and bottom temperature (e.g., reductions in ice extent and shrinking of the cold pool), and changes in circulation (stronger northward currents over the northeastern shelf in warmer years, particularly in 2018) led to changes in distributions of adult and age-1 pollock. Adult pollock were concentrated north of St. Lawrence Island and had larger longitudinal distributions in warm years, 2017–2019; whereas they had a more southerly and narrow distribution over the outer shelf in the cold year, 2010. Age-1 pollock had higher densities over the inner eastern shelf in 2017–2019 compared to 2010. Northward flow around St. Lawrence Island (particularly in the spring) alternated between stronger flow on the west side of the island in 2010 and 2017 and stronger flow on the east side of the island in 2018 and 2019; variations in flow may have impacted the location of prey and movement of feeding pollock to the Chukchi Sea. Size structure comparisons between NW, NE and SE sections of the Bering Sea shelf suggest that movement of fish between US and Russian waters may have been highest in 2019, one of the two warmest years, and lowest in 2010, the coldest year. Spatial comparisons of distributions and size structure across the Bering Sea help

provide a comprehensive view of factors affecting the movement of this highly important commercial fish species.

Key words: Walleye Pollock, Bering Sea, Temperature, Sea Ice, Cold Pool

1. Introduction

Movement of fishes in response to environmental conditions is a well-documented, adaptive response to maximize reproductive success, growth, and survivorship. Typical activating factors include a suite of environmental (temperature and salinity gradients, precipitation and runoff, fluctuating current regimes) and biological variables (e.g., prey resources, habitat optimization, predator and/or competitor avoidance, and mating and reproduction) that serve to initiate behavioral responses, either at the individual, population, or species levels. Climate change, particularly in the sensitive polar regions, exacerbates a number of these known drivers, prompting never-before-seen, population-level, spatial and distributional shifts (McLean et al., 2018; Mueter and Litzow, 2008). In the Pacific Arctic, large scale, northward movements of commercial stocks are underway as previously cold-dominated ecosystems warm and fish move directionally to higher latitude, relatively cooler environments. In the Bering Sea, such migrations have been recently documented among Pacific cod (*Gadus macrocephalus*), Pacific and Greenland halibut (*Hippoglossus stenolepis, Reinhardtius hippoglossoides,* respectively), and walleye pollock (*Gadus chalcogrammus,* hereafter pollock), (Kotwicki and Lauth, 2013; Spies et al., 2019; Stevenson and Lauth, 2019; Vestfals et al., 2016). In particular, shifts in the distribution of pollock are of special concern, as pollock in the eastern Bering Sea and Aleutian Islands (SE and NE shelf, Fig. 1) are the top US commercial fishery by biomass yielding over 1.3 million metric tons annually in recent years (2014-2017) (Fissel et al., 2019). In the western Bering Sea (including the NW shelf, Fig.1) Russian pollock yearly yields are lower, ~ 0.4 million metric tons (Khen et al., 2013), but are still a highly important fishery. In addition to their economic importance, pollock are also a key ecological component of the Bering Sea food web across the shelf, serving as a critical link between lower (zooplankton) and upper (fish, seabirds, mammals) trophic levels (Buckley et al., 2016).

Adult and juvenile pollock distributions over the SE shelf have varied between cold, high seasonal sea ice (hereafter, ice) years and warm, low ice years over a 38-year time series (Kotwicki et al., 2005; Kotwicki and Lauth, 2013, Thorson et al., 2017). During cold years, an extensive "cold pool" forms on the eastern Bering Sea shelf below the pycnocline and persists through the summer. Although the cold pool is commonly defined as temperatures below 2°C (e.g., Stabeno and Bell, 2019; Wyllie-Echeverria and Wooster, 1998), here, we use a cutoff of 0°C (termed 0°C cold pool in this manuscript), because adult pollock usually do not form feeding aggregations at temperatures below this threshold in the eastern Bering Sea (Baker, *in press*). Oceanographically, the eastern shelf has been classified into inner (< 50 m), middle (50–100 m) and outer (100-200 m) domains, each separated by an oceanographic front (Coachman 1986) (Fig. 1); the Aleutian Islands to 60°N, and 60°N to Bering Strait are considered to be the southern and northern Bering Sea respectively. Adults are typically located on the outer shelf outside (west) of the 0°C cold pool during cold years, with distributions spreading eastward toward the middle shelf in warm years (Baker, *in press*; Baker and Hollowed, 2014; Kotwicki et al., 2005). Age-1 pollock tend to be distributed more northerly than adult pollock and are likely less able to avoid the 0°C cold pool (e.g., Kotwicki et al., 2005; Thorson et al., 2017). Pollock over the NW shelf are typically observed off Cape Navarin in southern Anadyr Bay in cold or average years and also are limited by the 0°C cold pool located northeastward from this area, but spread farther north and northeastward in warm years. Multi-year, warm-cold oscillations of the environment and pollock distribution have been fairly typical over the last 15+ years (Stepanenko and Gritsay, 2016; Zuenko and Basyuk, 2017), though recent years (2018-2019) have been extremely warm (with bottom temperatures anomalies of ~ + 3–4 °C on the northern middle shelf at mooring 8, southwest of St. Lawrence I), and characterized by a lack of sea ice during winter (Stabeno and Bell, 2019), a heretofore unprecedented event. Lack of winter ice has led to a cascade of observed ecosystem changes across multiple trophic levels (Duffy-Anderson et al., 2019; Huntington et al., 2020). During and just prior to this period (2017–2019), summer distributions of adult pollock also changed considerably, with large population biomass observed in the northern reaches of the Bering Sea (north of St. Lawrence Island and in northern Anadyr Bay).

Changes in summer pollock distributions are likely related, at least in part, to the extraordinary changes in sea ice and water temperature in the Bering Sea. The summer cold pool extent is determined by late winter ice extent (Wyllie-Echeverria and Wooster, 1998) and recent reductions in ice cover have drastically decreased the extent of the cold pool. In particular, 2018 and 2019 exhibited the smallest cold pool extent observed in at least the last two decades (Basyuk and Zuenko, 2019; Danielson et al., 2020; Overland et al., 2019; Stabeno and Bell, 2019). Retraction of the cold pool may be key to pollock northward distribution. Historically, the cold pool (< 0°C) was avoided by migrating adults. This effectively served as a barrier to fish passage from the southern to the northern Bering Sea. Profound, climate-mediated shifts in ice dynamics, coupled with associated oceanographic changes, may be altering this division, potentially creating a new paradigm of pollock dynamics across all reaches of the Bering Sea. For example, during fall and winter as ice is forming in the northern Bering Sea, pollock move south to continue feeding in warmer areas. Accordingly, in years with reduced ice extent, there may be less incentive to move to the most southern areas where their traditional spawning grounds are located. Early ice retreat and warmer temperatures during winter can also lead to earlier spawning and an earlier start of feeding migrations (Kotwicki et al., 2005). Changes in hydrography can lead to changes in currents, which then have large impacts on planktonic prey resources for adults (which follow prey) and on juvenile pollock (e.g., age-0 and age-1) and other forage fish species, that are smaller and more susceptible to current flow.

Mean flow on the eastern Bering Sea shelf is weakly (< 0.05 m s^{-1}) northwestward (Fig. 1 Inset), along the shelf (e.g., Kinder and Schumacher, 1981; Coachman, 1986). The stronger Bering Slope Current (> 0.10 m s^{-1} during winter) flows northwestward along the shelf-break, closer to the shelf-break during winter and farther off-shelf during spring and summer (Ladd, 2014). The Bering Slope Current splits in the northern Bering Sea with most of the flow feeding the southwestward flowing East Kamchatka Current, while a small part of the flow moves onto the shelf toward Anadyr Bay and ultimately Bering Strait (Stabeno and Reed, 1994; Panteleev et al., 2011). This northward flow from Cape Navarin toward Bering Strait is known in Russia as the Navarin Current (Luchin and Menovshchikov, 1999). The turn to the north is associated with the density gradient between the low-salinity cold pool and the dense, high salinity cold water near the Chukotka coast, formed during winter ice formation. The Navarin Current is the only strong flow that penetrates deeply onto the shelf.

Historically, pollock distribution over the SE shelf is characterized by spatial separation of cohorts, which reduces competition among younger age classes for zooplankton prey, and minimizes cannibalism of younger stages by piscivorous adults (Duffy-Anderson et al., 2003). For example, age-1 pollock (unlike adults) are not able to perform long distance migrations (Kotwicki et al., 2005). Therefore, during their first winter age-1 pollock may not be able to migrate to ice free areas (as adults do), but instead many of them overwinter under the ice and stay in the cold pool throughout the summer. Adults avoid the cold pool, which results in a narrower spatial distribution. A result of this dynamic is a reduction in cannibalism of adults on age-1 pollock during cold years. Separation occurs in both the vertical and horizontal dimensions, and is precipitated by predation dynamics, differences in temperature tolerance, ontogenetic factors, diel shifts, and feeding and diet differences. On the NW shelf, however, spatial separation of pollock cohorts is absent; both adults and juveniles feed in the same area, though often in separate aggregations (Stepanenko and Gritsay, 2016). Climate-mediated shifts in ice and cold pool dynamics could alter the spatial partitioning for both the eastern and the NW Bering Sea, disrupting established feeding, refuging, and migrations across cohorts.

In order to fully assess the potential for broad-scale changes in pollock distribution over the Bering Sea and environmental factors driving these changes, it is critical to evaluate distributions across the entire shelf in both US and Russian sectors. The NOAA Alaska Fisheries Science Center (AFSC) bottom trawl survey now has 4 years of sampling (2010, 2017, 2018, and 2019) in the NE Bering Sea in conjunction with the ongoing annual sampling (1982-present) in the SE Bering Sea. These surveys are used to evaluate adult (age-4+) and juvenile (age-1) pollock distributions. The Pacific branch of Russian Research Institute of Fisheries and Oceanography (TINRO) has conducted similar bottom or midwater trawl surveys on the NW Bering Sea shelf since 1986, including the same 4 years. Our goal is to compare summer distributions and size structure data from SE, NE and NW shelf waters for these years, to decipher the extent of the pollock movement among these regions, and the environmental factors that influence these distributions. We lack information on large scale pollock distributions for seasons other than summer, therefore we are unable to fully evaluate the impact of environmental factors on winter, spring or fall distributions.

Three main questions will be addressed:

1) How do adult and age-1 pollock summer distributions vary across the Bering Sea shelf in high-ice/cold (2010) compared to recent intermediate and low-ice/warm (2017-2019) years?
2) How do environmental factors (ice, water temperature, currents) influence the summer adult and age-1 distributions?
3) Are population size structures similar for US (SE and NE) and Russian (NW) collected pollock (suggesting mixing of the US and Russia origin populations)?

Our evaluations are intended to allow fisheries managers and commercial fishers to gain a better understanding of current changes in stocks and potential factors driving these changes.

2. Methods

2.1. Survey data

Pollock were sampled in 2010 and 2017–2019 on bottom trawl surveys (primarily) during summer months (June-August, Table 1) over the SE, NE and NW Bering Sea shelf (Fig. 1). Timing of the SE and NE surveys was consistent among years. The SE surveys were conducted in June through July with sampling starting with the easternmost stations within Bristol Bay and progressing westward toward the Bering Sea continental slope edge (depths > 200 m) and the US-Russia transboundary line. Sampling for the NE surveys were scheduled to start after the completion of SE survey and a port call to Nome, AK, to re-provision the vessels. NE survey sampling occurred during the first 2–3 weeks of August with a north-to-south progression. The timing of NW surveys varied more, in particular the 2017 survey was conducted in June through July, whereas surveys in the other years occurred from mid/late July to mid-August/early September. Therefore, survey timing overlapped most for the NE and NW surveys in 2010, 2018 and 2019 and for the SE and NW surveys in 2017. Measurements of water temperature were collected at all trawl stations. We lacked the data (e.g., higher temporal resolution data on pollock distribution outside of our survey date) to normalize the trawl data to a specific date (unlike the bottom temperature, described in 2.2.1. below). However, surveys were planned to take into account the timing of pollock movements, and therefore provide a general picture of fish distributions. The differences in survey timing described above can be used to understand finer scale differences among years and regions.

2.1.1. SE and NE bottom trawls

Bottom trawl survey data have been collected by the NOAA AFSC Groundfish Assessment Program on the SE Bering Sea shelf annually during the summer since 1982 (Fig. 1). The survey is based on a systematic design consisting of 376 fixed sampling stations located in the center of 37.04 x 37.04 km (20 x 20 nautical mile) grid squares with the survey ranging from 54.5°N to 62°N latitude and bounded by the 20 m and 200 m isobaths and the US – Russia Convention line to the northwest. Bottom trawl survey data using the same methods were collected in the NE Bering Sea in 2010, 2017, 2018, and 2019. The NE Bering Sea shelf survey was designed as a continuation of the same systematic design established for the SE shelf survey, effectively extending sampling to 65.5°N latitude (Fig. 1). Note that in 2018 the survey extent and station spacing in the NE Bering Sea were non-standard, grid spacing was 30 nm (55.6 km) instead of 20 nm (37 km), and the Norton Sound region was not sampled. Sampling from the bottom trawl surveys in the SE and NE Bering Sea followed standard methods developed by AFSC (Lauth, 2011; Lauth et al., 2019; Stauffer, 2004). Vessels were equipped with 83-112 eastern otter trawls, which have a 25.3 m headrope, 34.1 m footrope, and a 32 mm liner in the codend to aid in retaining smaller animals. The mean effective opening of the trawl is 16.6 m horizontally and 2.7 m vertically.

Catch sampling followed standardized procedures described in detail by Wakabayashi et al. (1985) and Stauffer (2004). Catches with a total weight of 1,150 kg or less were sorted and weighed in their entirety, whereas larger catches were randomly subsampled. Fishes were identified and sorted to species to the extent possible, weighed, and counted. For the predominant fish species encountered, including pollock, a random subsample was weighed, sorted by sex, and measured to the nearest centimeter (cm) fork length (FL). Relative abundance was calculated by determining the catch-per-unit-effort (CPUE). CPUE values from each survey are provided for age-1 and adult pollock and were calculated as total weight (kg) per km^2. Based on the results of pollock aging studies, fish were assumed to be age-0 at < ~10 cm FL, age-1 at 10–19 cm, age-2/3 at 20–34 cm, and age-4+ adults at ≥ 35 cm (Kimura et al., 2006). Note that the majority of pollock < 35 cm are less than 4 years old (Fig. A.1), and are not consistently caught with the US gear (83-112 eastern otter trawl), with the exception of age-1s (Lauth, 2011).

Temperature and depth profiles were collected using a Sea-Bird Electronics (SBE) 39 datalogger that was attached to the headrope of the trawl. Observations were collected at 3-second intervals during the full duration of each tow. Mean bottom temperature was calculated as the mean temperature sampled between on- and off-bottom events, determined by the bottom contact sensor for each tow.

2.1.2. NW bottom and acoustic/midwater trawls

Bottom trawl data were collected in 2010, 2017, 2019, and a midwater trawl survey coupled with an acoustic survey was conducted in 2018 on the NW Bering Sea shelf and continental slope with bathymetry < 500 m (Fig. 1). There was no survey in Anadyr Bay in 2019. The bottom trawl gear consisted of a DT-27.1/24.4 net with a horizontal opening of 16.26 m, vertical opening of ~3.6 m and a 10 mm mesh cod end (Savin, 2011). The midwater trawl RT/TM-80/396 had a 40 m opening and a 8 m cod end with 10 mm mesh; the layer from 350 m depth or from the shelf bottom to the sea surface was fished. Acoustics were done with an echo sounder SIMRAD EK-60, using the operating frequencies 38 and 120 kHz; the data were processed with SIMRAD software, with quantitative estimations based on the 38 kHz signals.

For bottom and midwater trawls, every catch was sorted and weighed entirely. Fishes and invertebrates were identified and sorted to species to the extent possible, weighed, and counted. For the predominant fish species encountered, including pollock, a random subsample was weighed, sorted by sex, and measured by centimeter intervals of fork length. Pollock density distribution was estimated following standard methods (Savin, 2011, 2018).

Temperature and salinity data were collected from CTD profiles using a SBE-19plus or SBE-25 deployed to the sea bottom at each station, immediately after trawling. All CTD data were processed with SBE software following standard methods and binned into 1-m bins. Bottom temperature was estimated as the deepest value of the profile.

2.2. Data analysis

2.2.1. Environmental variables

Environmental variables evaluated include sea-ice concentration during the preceding winter, summer bottom temperature, and spring and summer modeled bottom currents for 2010, 2017, 2018, and 2019.

Sea-ice maximum extent and timing of retreat were evaluated using satellite measurements from NOAA/NSIDC Climate Data Record of Passive Microwave Sea Ice Concentration, Version 3 (Meier, et al., 2017; Peng et al., 2013) downloaded from the Alaska Ocean Observing System (AOOS) data portal (portal.aoos.org). Ice retreat timing was calculated as the day of year when ice concentration in each pixel reached (and remained) less than 30%. Winters 2009/2010, 2016/2017, 2017/2018 and 2018/2019 were designated as 2010, 2017, 2018 and 2019, respectively.

Bottom temperature data from the SE, NE and NW shelf surveys were combined. The total number of temperature profiles varied from 532 in 2018 to 957 in 2010 (Fig. A.2). The following procedure was used to estimate synoptic (normalized to July 15) bottom temperature from the surveys (data collected at different survey dates): 1) climatological bottom temperatures ($T_{clim}(x_i,y_i,t_i)$) were estimated from the World Ocean Atlas 2013 (WOA2013) version 2 monthly climatology (Locarnini et al., 2013) using linear interpolation; 2) for each measurement ($T_i(x_i,y_i,t_i)$), an anomaly from the interpolated climatology was calculated for the observed date and location ($T_{anom}(x_i,y_i,t_i)= T_i(x_i,y_i,t_i)-T_{clim}(x_i,y_i,t_i)$), thus removing any effect of the timing of observation; 3) bottom temperatures were then normalized to July 15 as the sum of the July 15 climatological value and the anomaly ($T_{norm}(x_i,y_i,15\ July)= T_{clim}(x_i,y_i,15\ July)+ T_{anom}(x_i,y_i,t_i)$).

Mean bottom currents for spring (March, April, and May average) and summer (June, July, and August average) over the Bering Sea shelf were examined using output from a regional ocean-sea ice model in the Bering Sea with 10 km horizontal resolution (named Bering10K hereafter).

Bering10K is based on ROMS (Regional Ocean Modeling System) (Haidvogel et al., 2008), a terrain following vertical coordinate ocean general circulation model with tides, and is coupled to a dynamic-thermodynamic sea ice model (Budgell 2005). Over the time period of examination, Bering10K is forced by prescribed surface atmosphere and ocean lateral boundary conditions from NOAA Climate Forecast System Reanalysis (CFSR) and its operational extension (CFSv2-OA). CFSR and CFSv2-OA are reanalyses products where a suite of satellite and in situ observations are assimilated into a coupled climate model (Saha et al., 2010); as such, they represent a best estimate of past historical climate conditions. The transport through the northern boundary (Bering Strait) is relaxed to the observed value of 0.8 X 10^6 m^3 s^{-1} (Woodgate and Aagaard, 2005); sensitivity studies tested whether a seasonally varying open boundary condition could better replicate flow patterns in the northern portion of the domain, but the simple relaxation condition was found to perform equally well (Kearney et al., 2020). Bering10K modeling framework and detailed model evaluation are provided in Kearney et al. (2020).

2.2.2. Pollock distribution and size structure

The pollock distribution data were combined from US (SE, NE shelf) and Russian (NW shelf) surveys. Prior to combining data, the US data were corrected for density dependent efficiency of the survey bottom trawl (Kotwicki et al., 2014). The correction was applied using formula $CPUE_o/q$ where $CPUE_o$ is observed CPUE and q averaged 0.75 across years used in analysis and ranged between 0.73 and 0.77. This correction was applied because it has been established that corrected estimates are less biased and more precise with respect to the mean CPUE and variance (Kotwicki and Ono, 2019). The Russian data were not corrected, because in years used in analysis we did not have data that could be used to compare efficiency of the US and Russian survey bottom trawls. However, data from years 1982–1990, when both Russian and US surveys were conducted over the SE shelf suggests that the median sampling efficiency ratio for the Russian survey relative to the US survey for pollock biomass was 0.7 ± 0.16 (O'Leary et al., *in review*). Because bottom trawl efficiency values in the past were close and we do not have data to estimate these values for the recent surveys we decided that the best approach was to not correct Russian CPUE data. Adult distribution maps were plotted in the biomass units (kg km^{-2}), but juveniles (age-1) were plotted in abundance units (number km^{-2}) because of the highly variable weight of juveniles. Maps of pollock distribution overlain with bottom temperature contours (0°C and 6°C) were made with ArcMap (version 10.3,2014, ESRI, Inc.) by inverse distance weighting CPUE data (kg/ha) for adult and age-1 pollock in each survey year for the SE and NE shelf. The preferable bottom temperature and bottom depth range for adult and age-1 pollock was evaluated by comparing mean proportions of pollock abundance relative to bottom temperature and depth for data collected in the SE and NE Bering Sea from 1987 to 2019. We were unable to perform these analyses for pollock collected on the NW shelf.

Pollock size distribution data were plotted as histograms for the three areas of the Bering Sea shelf. Percent frequency of occurrence (proportion of individuals) was plotted for each 1 cm length bin. In 2018, size structure was determined only for the NE and SE Bering Sea shelf since the NW pollock data were collected with midwater trawls, which likely collect smaller fish than bottom trawls and could bias the size estimates for comparison. Note that in 2019, the NW fish collection was limited to the Koryak shelf and Cape Navarin (southern part of NW shelf, Fig. 1).

3. Results

3.1. Environmental variables

Of the four years (2010, 2017, 2018, and 2019), maximum sea-ice extent was greatest in the winter of 2010, followed by 2017 (Fig. 2). Maximum extent was comparable in the two years 2018 and 2019 in the eastern Bering Sea. However, on the NW shelf (Anadyr Bay), 2018 exhibited a notable lack of sea-ice compared with the other years. The timing of sea-ice retreat at a given location was much earlier in 2018 and 2019, followed by 2017, then 2010 (Fig. 3). For example, ice retreated southeast of St. Lawrence Island in April 2018 and 2019, May 2017 and June 2010.

Bottom summer temperature data (normalized to July 15) show the cold pool extended into the southern shelf in 2010 and 2017, but not in 2018 or 2019 (Fig. 4). Water colder than 0ºC was almost nonexistent in 2018 and was limited to south and west of St. Lawrence Island in 2019. In 2017, on the southern shelf, the water colder than 0ºC was limited to a small area compared to 2010 when the low temperatures extended over almost the entire middle shelf. Bottom temperatures were extremely warm (12–15°C) along the eastern Inner Domain in 2017, 2018 and 2019, but ≤ 10°C in the same region in 2010. Otherwise, temperatures in 2010 remained < 2°C, aside from small areas in outer Anadyr Bay (2.5°C), just north of St. Lawrence Island (3°C), and outer Norton Sound (2–3°C). In 2017 and 2019, larger areas with higher temperatures were observed in Anadyr Bay, north of St. Lawrence Island and in Norton Sound. Data were not available for 2019 in Anadyr Bay.

Bottom currents on the northern shelf from Bering10K show that the strongest spring (March, April, May) and summer (June, July, August) currents (> 5 cm s^{-1}) in all years were found NW of St. Lawrence Island and in Bering Strait (Figs. 5, 6). In the spring, northward flow between St. Lawrence Island and the Chukotka Peninsula was strongest in 2010 and 2017 while flow on the east side of St. Lawrence Island was stronger in 2018 and 2019. During summer, flow west of St. Lawrence Island was strongest in 2017 while east of the island, flow was weaker and did not exhibit the same interannual variability as observed in the spring.

In Anadyr Bay during both spring and summer, flow into the Bay (toward the northwest) was strongest in 2017, feeding the flow around the Chukotka Peninsula toward Bering Strait. During spring, flow was predominantly out of the bay (toward the southeast) in 2018 and 2019. In 2010, spring flow was weak and spatially variable in the bay but stronger across the bay mouth (toward the northeast). During summer, flow in all years was predominantly directed into the bay but stronger on the southwest side.

3.2. Pollock distribution and size structure

Adult pollock distributions during summer varied among years across the Bering Sea shelf (Fig. 7). In 2010, the pollock were found in high concentrations (> 10,000 kg km^{-2}) in the outer shelf from the middle front to the shelf break (100-200 m bathymetry), and in patches north of Unimak Island in the south and outside of Anadyr Bay on the NW shelf (Fig. 7). In 2017 the adult pollock were more widespread across the shelf with high concentrations in western Anadyr Bay and north and west of St. Lawrence Island up to Bering Strait with smaller patches south of the island. In 2018, there was a low abundance of pollock on the SE shelf with small high density patches north of the Aleutians and near the Pribilof Islands; the highest concentrations were found on the northern outer shelf, and north and west of St. Lawrence Island to the Bering Strait, the northern limit of the available bottom trawl survey data. Acoustic data for the NW shelf in 2018 also indicate high densities of pollock south and west of St. Lawrence Island at the mouth of Anadyr Bay (Fig. 8). In 2019, the adults were found over most of the outer and middle shelf with high concentrations also south of Bering Strait. Since there was no 2019 survey in Anadyr Bay, concentrations in that region could not be evaluated.

The adult distributions appear to relate to the seasonal coverage of sea-ice and bottom temperature. In the high and moderate ice years of 2010 and 2017, respectively, the adults were located outside (west) of the 0°C cold water region (Figs. 4, 7; Fig. A.3). Whereas, in the very low ice years (2018 and 2019) with almost no bottom water colder than 0°C, the adults were more evenly distributed over the middle and outer shelf. However, these fish were not found in temperatures above 6°C (Figs. 4, 7; Fig. A.3); thus, distributions in these years may have been constrained by high rather than low temperatures. A comparison of bottom temperature and depth range for adults in the eastern Bering Sea for 1987 to 2019, indicates that most adults are found at temperatures of 0-6°C. On average only about 2.5% of adults were found below 0°C and less than 1% above 6°C (Table 2). Overall, cross-shelf distributions were larger (extended over a greater depth range) in warm than in cold years. The high adult concentrations located north of St. Lawrence Island and in the NW region in 2017–2019 coincided with areas of higher bottom temperatures. Additionally, high concentrations of pollock were found on the northern middle shelf between St. Matthew and St. Lawrence islands in 2019.

General patterns of the adult distribution in the NW and NE regions may partially relate to the summer currents. In 2010, 2017 and 2018, high concentrations of adults were present in western Anadyr Bay potentially following the Navarin Current. Concentrations of adult pollock were also high to the west and north of St. Lawrence Island toward Bering Strait in 2017–2019, in the region of high currents. In the NE, adult pollock densities were much lower in 2010 compared to the 2017–2019, while in the NW there was not much difference in pollock densities between these periods.

Age-1 pollock tended to have a more northerly distribution than adults (Figs. 9, 7). In 2010, age-1 pollock were generally in higher concentration (> 1000 km^{-2}) in the outer shelf, but not as far offshore as adults, with smaller patches in the middle shelf, similar to adults, but also had high concentrations in Anadyr Bay (Fig. 9). In 2017, age-1 pollock were found in similar locations on the SE outer shelf and in Anadyr Bay, but were also located on the eastern inner shelf between

Nunivak and St. Lawrence islands. In 2018 and 2019 (the years with stronger northward flow east of St. Lawrence Island), age-1 pollock had a larger cross shelf distribution with the high concentrations located near the eastern inner shelf particularly in 2019 (large area with > 10,000 pollock km^{-2}). Fewer age-1 pollock were observed in Anadyr Bay in 2018; there was no survey within Anadyr Bay in 2019, although there is an indication of high concentrations of age-1 pollock south of this area.

Age-1 pollock were found over a greater bottom temperature range than adults (Table 2, Fig. A.4). Some age-1 fish were found in temperatures < 0°C, although the highest concentrations were found outside of the 0°C cold pool. Age-1 pollock on the eastern inner shelf in 2018 and 2019 were found in warm (10°C) water, much higher than the 6°C temperature limit for adult distributions. On average age-1 pollock appear to be more widely distributed across bottom temperatures and depths, as indicated by an average 5.7% of age-1 pollock distributed in waters below 0°C, and 6.7% in waters above 6°C (Table 2). The high concentrations of age-1 pollock over the eastern inner shelf in 2018 and 2019, in particular, were located in an area with notable northward bottom currents (1-4 cm s^{-1}) south and east of St. Lawrence Island during spring (March–May) (Figs. 9, 5). Age-1 pollock were not found in this eastern inner shelf area in 2010 when spring (and summer) northward bottom currents were low.

Pollock size structure data indicate differences in several year classes/age groups in the NW compared to SE and NE fish; this is particularly evident in 2010 and 2017 (Fig. 10). For example, in 2017 in NW pollock, there were 5 distinct modes in length frequency histograms at ~13, 21, 28, 39, and 48 cm. Only modes similar to the first and last high modes for NW fish were seen in the NE fish at 15 and 49 cm, and in the SE fish at 15 and 45 cm. Age-1 pollock (~ 10–20 cm, Kotwicki et al., 2005) were found in all regions (NW, NE, and SE) in all years (2010, 2017, 2018, and 2019); the percentage of age-1 pollock were highest in 2010 in the NW and NE, and in 2019 in the NE. In 2010, the cold year, a 40 cm mode was observed both in the SE and NW. Each warm year (2017, 2018, and 2019) appeared to have a different pattern among regions in the size of the largest fish (> 35 cm). In 2017, all 3 regions had main modes from 40–50 cm, but in the NW there was an additional mode at 39–40 cm. In 2018, the main mode in the NE was larger than in the SE (51 compared to 44 cm), and in 2019 all regions have similar size structure with the main mode at 46–48 cm and minor modes at 23–25 cm. Spatial differences in size structure were observed even within areas. For example, the two modes for adult pollock in the NW area in 2017 reflect the spatial inhomogeneity of size structure within this area. The relatively small fish with the dominant size 39–40 cm were numerous in its southern part (on Koryak shelf), whereas the fish > 50 cm strongly prevailed at Chukotka coast in the northern Anadyr Bay. Possibly, these two peaks were formed by fish with the same age, but different origin. The same main size group of adults (age-4+ fish, last mode) is observed in all 3 areas in all years, with exception of the NE in 2010 where it was totally absent.

4. Discussion

4.1. Environmental factors related to changes in pollock distribution

Recent changes in adult and age-1 summer pollock distributions in the Bering Sea appear to be related to changes in climate including ice cover, water temperature, and oceanographic currents. Like others have reported earlier, our analyses of US collected data suggest that during cold years when ice is present and extensive, adult pollock are constrained to the outer Bering Sea shelf, limited by the presence of the frigid bottom waters of the 0°C cold pool (Kotwicki et al., 2005). During warm years when ice is lacking and the cold pool is negligible or absent, pollock are unconstrained by cold bottom temperatures and they shift their distributions northward. However, unique to this study are the inclusion of northwestern Bering Sea (Russian) derived data that demonstrate that not only are pollock distributions north-shifted after ice-reduced winters, but there appears to be more intensive mixing between the Russian stock as it moves north and eastward, and the US stock as it moves north and westward. Specifically we show that pollock expanded their distribution to the area between St. Matthew and St. Lawrence islands in the US, and the area between St. Lawrence Island and Bering Strait in both US and Russian waters. Russia – US stock mixing could portend changes in stock diversity, which has important implications for pollock population resilience, rebuilding, and recovery in the face of climate shifts and anthropogenic pressures.

Several atmospheric and oceanographic factors acted in concert to prompt the spatial shifts described above. Changes in winds during winter impacted the ice and currents in 2017–2019. The seasonally averaged wind anomalies for 2014–2018, compared to 1979–2013, indicate that winds from the south (toward north) were much more prevalent in winter and fall in 2014–2018 (Danielson et al., 2020). These northward winds were correlated to northward water flow in Bering Strait (Danielson et al., 2020), and promoted northward movement of ice (Stabeno and Bell, 2019). In winter 2018, winds from the south occurred in November 2017, and again in February 2018, whereas in winter 2019, more typical winds from the north (and typical ice conditions) occurred in December–January, followed by the return of winds from the south in February 2019 (Stabeno and Bell, 2019). The ice responded to these wind patterns with more ice present in early winter in Anadyr Bay in winter 2019 than in winter 2018, although ice was low elsewhere in the Bering Sea in both winters.

We hypothesize that in 2017, the pollock moved north from their spawning locations over the SE shelf to the NE and NW shelf, stayed farther north than normally over winter due to the low ice conditions, particularly the lack of ice in Anadyr Bay, and remained there in summer 2018 leading to large numbers north of St. Lawrence Island and on the NW shelf, and exceptionally small numbers of pollock in the SE in 2018 (Ianelli et al., 2019). In autumn-winter 2018/2019, adults preferentially moved south as ice concentrations in Anadyr Bay returned to normal in early winter. This may have led to fewer adults north of St. Lawrence Island and more adults in the SE Bering Sea in 2019 compared to 2018 and 2017 (Ianelli et al., 2019). Bottom temperature was shown to be the most significant predictor of pollock distributions for the 1982–2018 time series in the eastern Bering Sea; variables tested included temperature (bottom, surface, minimum, maximum, and range), depth, stratification, substrate, latitude, and longitude. (Baker, *in press*). Baker (*in press*) also found that pollock were associated with a bottom temperature range of 0 – 4°C.

The high temperature band along the eastern Bering Sea inner shelf in very warm years, 2019 in particular, may limit adults from moving inshore. The increase in metabolic rates at higher temperatures requires pollock to consume more food to avoid starvation and maintain feeding and growth (Smith et al., 1988). The inner shelf varies from the middle and outer shelf ecosystems with differences in taxa and size of zooplankton and forage fish; for example, the inner shelf has smaller-sized and fewer lipid-rich zooplankton taxa (Eisner et al., 2014) and younger/smaller stages of forage fish such as Pacific herring (*Clupea pallasii*) (Andrews et al., 2016). Therefore, adult pollock may avoid or not survive on the inner shelf due to temperature limitation, low prey/food availability or a combination of these or other factors. The presence of age-1 pollock on the inner shelf may reflect the ability of juveniles to tolerate a larger temperature range than adults, as well as differences in preferred prey for adults and juveniles (Buckley et al., 2016). Pollock in the eastern Bering Sea have been shown to move from nearshore to offshore habitats as they progress from juvenile to adult stages (Baker, *in press*; Barbeaux and Hollowed, 2018; Hollowed et al., 2007).

We also hypothesize that heightened air and sea surface temperature in the northwestern Bering Sea in winter 2018 prevented the water column temperature from becoming cold enough to form a dense lens of water (cold pool) at the shelf bottom. In addition, the stratification was weak in the spring due to the lack of fresh water from ice melt, so the surface warmth could mix deeper, eroding whatever cold pool had formed over the winter/spring (Stabeno and Bell, 2019). As a result, the Navarin Current, usually a strong northeastward flowing current in summer (Favorite et al., 1976; Luchin and Menovshchikov, 1999; Stabeno et al., 2016), was weaker compared to other warm years or sometimes absent. Instead, a northward stream developed that flowed along the eastern shelf and passed east of St. Lawrence Island (Fig. 5). This circulation change likely resulted in a change in pollock summer migration patterns by assisting them to move toward the Chukotka coast using both the Navarin Current and this along-shelf northward stream, as indicated by observations of dense aggregations of pollock in the southern and northern parts of Anadyr Bay (Fig. 8). Accordingly, dense feeding aggregations of pollock were observed at bottom depths throughout Anadyr Bay in 2017–2018 (bottom trawl survey data for 2017 and acoustic survey data for 2018), though their density in the midwater was still lower in the northern part.

4.2. Indications of movement of pollock among regions based on size structure

Size structure data can be used to estimate similarity (and potential mixing) of populations among the SE, NE and NW regions over our 4 study years. In general, the NE and NW have similar modes (first mode indicative of age-1 fish and last mode indicative of age-4+ fish) for all years. General size structure in the Russian sector (NW) is not similar to that in the US sector (SE and NE) in 2010, because of additional minor modes observed in the NW. This suggests that the pollock present in the northeastern part of the Russian EEZ in summer were a mixture of several stocks that originated from the eastern and western spawning grounds. Kotwicki et al. (2005) hypothesized that timing of feeding migrations is earlier in warm years compared to cold years, which can result in summer distributions that are farther north in warm years compared to cold years. If this is the case, in warm years in the NW and NE we may observe pollock stocks that are more mixed compared to the cold years. Additionally, larger fish can move faster (Kotwicki et al., 2005), leading to slightly larger fish in the north than south. An interesting feature of the pollock length data is a broader size distribution for modal groups for the NW shelf. The US bottom trawl surveys typically only capture age-1 and small numbers of very old and large fish in the 0°C cold pool. Therefore, the size structure shown in the NE in 2010, where pollock in this region were almost entirely observed within the 0°C cold pool, is not unusual. Without the cold pool present, pollock distribution demographics may be similar across the international border as suggested by the similar size structure in all regions in 2019. Some of the differences between the NE and NW in the presence or absence of the modes for 2 and 3 year old pollock likely arise from low selectivity of the US bottom trawl survey for these ages (Ianelli et al., 2014). The US bottom trawl survey does not consistently capture age-2 and age-3 pollock because these pollock are often located above the depth of the bottom trawl headrope as demonstrated by higher relative catches of age-2 and age-3 pollock on acoustic surveys (Honkalehto et al., 2013). Differences in the trawl gear (e.g., bottom trawls on Russian surveys have a 3.6 m vertical opening compared to 2.7 m for US surveys) or differences in the depth distribution of the age-2 and age-3 populations can confound interpretation of the size structure data between US and Russian surveys.

4.3. Spawning and feeding migrations

It is unknown whether population-level movement of Bering Sea pollock in response to changing temperatures and ice are temporary shifts that may be reversed if cold stanzas return to the Bering Sea shelf, or whether they are indicative of broader, enduring range alternations that include colonization of higher latitude areas. Pollock are known for their ability to change spawning locations depending on environmental conditions. For example, within the eastern Bering Sea, during warm springs, pollock spawning occurs more to the east (on the middle shelf) while during cold years it is to the west (outer shelf) (Smart et al., 2012). Also, connectivity between spawning and nursery areas is higher during warm years, maximizing dispersal potential

(Petrik et al., 2016). Evidence of colonization would include indication of gonad development in adult fishes (spawning condition), and multi-year collections of eggs and early-stage larvae (yolk sac). At present there are comparatively few records of early-stage pollock larvae being collected in the northern Bering and Chukchi seas so it seems unlikely that northern colonization on a large scale has occurred. However, a historic paucity of field sampling during the spawning months (~March–June) in the northerly reaches of the shelf precludes a conclusive assessment. Of those larvae that have been collected, it seems most likely that they were transported from known (Unimak, Bogoslof, or Pribilof islands; Bacheler et al., 2010) or purported (Zhemchug or Navarin canyons) spawning areas rather than being locally produced. Theoretical biophysical transport modeling efforts have demonstrated that pollock larvae spawned from the northern-most known spawning areas in the eastern Bering Sea connect significantly with nursery habitats over the middle and outer shelves in the northern Bering Sea (Petrik et al., 2016), though connectivity from known spawning regions to the Chukchi Sea has not been shown. Connectivity of older early life stages (age-0) to northerly regions is also theoretically possible; a combination of favorable currents and directional swimming could enable age-0 pollock to reach northerly regions of the Bering Sea in as little as 4-6 weeks (Duffy-Anderson et al., 2017). Pollock early life stages (< age-2) are unique from adult stages in that, because they have wide thermal tolerance ranges, they are capable of withstanding the frigid (-1.0 – 0°C; Laurel et al., 2015; Laurel et al., 2018) cold pool temperatures that adults avoid, making young capable of moving northward even during years when a sizable cold pool is present. However, extensive population level migration such as that presented here requires a thermal corridor that permits the large-scale exchange of multiple age classes of pollock, suggesting it can only occur during periods that are warm, ice-free, and cold pool minimal over multiple years.

Movement of fish not only requires appropriate environmental conditions, but also the right biological conditions as well. Of course, spatial scale is a critical issue in these considerations, with biotic controls exerting sizable influence over smaller scales and abiotic controls exerting influence over larger scales. One significant exception to this general observation is the large-scale seasonal migration (Kotwicki et al., 2005) that pollock undertake post-spawning (spring) to forage areas (summer) and then to overwintering grounds (fall/winter) which is likely motivated by both biotic (reproduction, feeding) and abiotic (temperature) controls. Nevertheless, all life history stages of pollock are able to modify their behavior to exploit food resources that maximize energy intake and growth and minimize predation risk. While not examined in the present study, the ability of prey (zooplankton) and predators (arrowtooth flounder (*Atheresthes stomias*), seabirds such as murres, and northern fur seals (*Callorhinus ursinus*)) to also modify their behavior in response to changing oceanographic conditions is a reasonable assumption. Pollock are zooplanktivores and preferentially prey on euphausiids and large, lipid-rich zooplankton species. Juvenile pollock have been previously demonstrated to shift their vertical distribution (Olla and Davis 1990; Schabetsberger et al., 2003) in response to shifting prey availabilities, and adults shift horizontal distributions in response to zooplankton occurrence (Barbeaux and Hollowed, 2018). Spatial shifts in pollock as related to predator avoidance have also been documented (Bailey, 1989; Ciannelli et al., 2002), as are shifts in response to presence of competitors (Sturdevant et al., 2001).

4.4. Value of evaluating data across E and W Bering Sea

The inclusion of data from both the eastern and western Bering Sea shelf, across the US–Russia transboundary line is imperative for understanding the movement of pollock and the underlying climatic, environmental and biological drivers for these distribution changes. This is especially relevant in recent warm years (with likely greater movements across international borders, as suggested by the similarity in size structures in 2019). The dramatic northward movement in 2017–2019 and range shifts in pollock also complicate evaluations of stock abundance and provide challenges for management of this large commercial fishery (Baker, *in press*). It is vitally important for researchers across the Bering Sea shelf to work together to address these recent and future variations in pollock distributions. Moreover, cross border issues are not limited to pollock, but also to other species such as Pacific cod, and flatfish (e.g. Alaska plaice (*Pleuronectes quadrituberculatus*); O'Leary et al., *in review*). Due to the differences in the survey and density estimation methodology between US and Russian surveys our comparisons of densities on both sides of the border are more qualitative than quantitative. However in the future it is important to improve on these estimates by improving cooperation between Russia and the US to focus not only on data sharing but also on comparisons of catchability and selectivity of survey gears used on both sides of the border. The precision and accuracy of across border fish movement estimates will depend on the ability to estimate accurate selectivity ratios between survey gears (Kotwicki et al., 2017). However, selectivity ratios can only be estimated from experimental paired sampling or by using nearest neighbor techniques (e.g. O'Leary et al., *in review*). Both of these methods require closer cooperation between US and Russian survey scientists. Good examples of such cooperation existed in the 1980s and 1990s, when it was common for Russian surveys to sample in the eastern Bering Sea; however this sampling has not occurred in the last two decades. Other examples of dedicated international survey efforts include the Russian-American Long-term Census of the Arctic (RUSALCA; Crane and Ostrovskiy, 2015) in the Chukchi Sea and the current Year of the Salmon surveys in the Gulf of Alaska. Continuation of long term monitoring efforts and increased cooperation between monitoring programs for groundfish and habitat variables (e.g., water temperature) by US NOAA and Russian TINRO scientists, will allow researchers to better monitor and understand impacts of climate change on the Bering Sea fisheries and ecosystems.

Coordinated efforts through international organizations (e.g., the North Pacific Marine Science Organization (PICES), the Pacific Arctic Group (PAG), and the North Pacific Anadromous Fisheries Commission (NPAFC)) are also crucial for ongoing communication, data synthesis and the sharing of research ideas and hypotheses. PICES efforts include the North Pacific Ecosystem Status Report, plenary presentations in Vladivostok, Russia in 2017 by Zuenko et al. and Kivva et al., and two workshops on international interdisciplinary efforts to understand the role of the North Bering Sea in modulating arctic environments (Eisner et al., 2017; Baker et al., 2018). Communication has been greatly strengthened by publication of collaborative research, such as Panteleev et al. (2011) on topography, Baker et al. (2020) and Danielson et al. (2020) on oceanography, Beamish et al. (1999) on pelagic fishes, Aydin et al. (2002) on food webs, and O'Leary et al. (*in review*) on groundfish spatiotemporal variations, in addition to the current manuscript.

4.5. Future considerations

Data presented here on warm-year shifts in pollock distribution between the southern and northern Bering Sea present several important points for consideration. First, are the observed changes presented here harbingers of the future? Ocean heating has already altered the southern Bering Sea shelf such that ice-free winters are now common (2001–2019) and associated warm-year cascading fisheries population and demographic shifts are expected; will the same be true of the northern Bering Sea? Our data show that Russian–US stock mixing over multiple years may be occurring, which can affect the demographic make-up of both populations. Moreover, thermally-mediated differences in age-specific survivorship also could be occurring, given age-selective processes previously described for pollock in the southern Bering Sea during warm stanzas (Heintz et al., 2013).

Stock shifts and stock mixing could pose other problems, as well. Homogenization and loss of diversity (portfolio effects) is known to decrease the ability of a population to adapt to changing conditions, heightening the risk of volatility and exacerbating the potential for failure. Likewise, local population extinctions in areas depleted by northward moving stocks are another topic of concern. Ecologically, local depletions increase the risk of imbalance in food web dynamics, with changes in energy transfer, and potential loss of other co-dependent species. Economically, local depletions of commercial stocks like pollock will require fishers to travel farther to harvest fish, with cascading consequences on cost, time, and resources (Haynie and Huntington, 2016).

Spatial analysis of pollock distributions over the 1982-2018 time series indicated that the highest variance in abundance was outside core habitat areas, suggesting that pollock are able to expand their ranges and utilize areas of more marginal habitat (Baker, *in press*). In 2018 and 2019 adult and juvenile pollock have been observed in high densities in the southern Chukchi Sea on fisheries oceanography surveys, both in the US and Russian sectors (E. Farley, A. Savin, pers. comm.; Orlov et al., 2020). This suggests that pollock have the potential to move northward from the north Bering Sea into the Chukchi Sea as the climate warms and ice diminishes. Whether it will be possible for pollock to colonize these Arctic regions remains an open question that depends, in part, on the magnitude of the climate change in the future, but also on the pollock temperature tolerance, prey resources, reproductive requirements, and predation pressure. Enhanced collaboration among US and Russian researchers is essential for successful evaluation of distribution changes and management of key Bering Sea fisheries in the face of a rapidly changing climate.

Acknowledgements

We thank the captains, crew, and scientific staff who participated on the many Bering Sea fisheries surveys conducted by NOAA AFSC (US) and TINRO (Russia). Funding for surveys and data analysis was provided by NOAA Fisheries, NOAA PMEL, and TINRO. This is PMEL contribution #5082. This is FOCI publication number XXX. We are grateful to PICES for encouraging the international collaborations that led to the production of this manuscript.

References

Andrews, A.G., Strasburger, W.W., Farley, E.V., Murphy, J.M., Coyle, K.O., 2016. Effects of warm and cold climate conditions on capelin (*Mallotus villosus*) and Pacific herring (*Clupea pallasii*) in the eastern Bering Sea. Deep-Sea Res. II. 134, 235-246.

Aydin, K.Y., Lapko, V.V., Radchenko, V.I., Livingston, P.A., 2002. A comparison of the eastern Bering and western Bering Sea shelf and slope ecosystems through the use of mass-balance food web models. NOAA Technical Memorandum NMFS-AFSC. 130.

Bacheler, N.M., Ciannelli, L, Bailey, K.M., Duffy-Anderson, J.T., 2010. Spatial and temporal patterns of walleye pollock (*Theragra chalcogramma*) spawning in the eastern Bering Sea inferred from egg and larval distributions. Fish. Oceanogr. 19, 107–120.

Bailey, K.M., 1989. Interaction between the vertical distribution of juvenile walleye pollock *Theragra chalcogramma* in the eastern Bering Sea and cannibalism. Mar. Ecol. Prog. Ser. 53, 205-213.

Baker, M.R. *in press*. Contrast of warm and cold phases in the Bering Sea to understand spatial distributions of Arctic and sub-Arctic gadids. Polar Biol.

Baker, M.R., Hollowed, A.B., 2014. Delineating ecological regions in marine systems: Integrating physical structure and community composition to inform spatial management in the eastern Bering Sea. Deep-Sea Res. II. 109, 215–240. https://doi.org/10.1016/j.dsr2.2014.03.001.

Baker, M., Kivva, K., Eisner, L., 2018. The role of the northern Bering Sea in modulating the Arctic II: International interdisciplinary collaboration. PICES Press, 26(1), 15-19.

Baker, M.R., Kivva, K.K., Pisareva, M.N., Watson, J.T., Selivanova J., 2020. Shifts in the physical environment in the Pacific Arctic and implications for ecological timing and conditions. Deep -Sea Res II. https://doi.org/10.1016/j.dsr2.2020.104802.

Barbeaux, S.J., Hollowed, A.B., 2018. Ontogeny matters: Climate variability and effects on fish distribution in the eastern Bering Sea. Fish. Oceanogr. 27, 1–15. https://doi.org/10.1111/fog.12229.

Basyuk, E.O., Zuenko Y.I., 2019. Bering Sea: 2018 as the extreme low-ice and warm year. Izvestia TINRO (Newsletters of Pacific Fish. Res. Center) 198, 119-142.

Beamish, R.J., Leask, K.D., Ivanov, O.A., Balanov, A.A., Orlov, A.M., Sinclair, B., 1999. The ecology, distribution, and abundance of midwater fishes of the Subarctic Pacific gyres. Progress in Oceanography 43 (2-4), 399-442.

Buckley, T.W., Ortiz, I., Kotwicki, S., Aydin, K., 2016. Summer diet composition of walleye pollock and predator–prey relationships with copepods and euphausiids in the eastern Bering Sea, 1987–2011. Deep-Sea Res. II. 134, 302–311.

Budgell, W.P., 2005. Numerical simulation of ice-ocean variability in the Barents Sea region. Ocean Dynamics, 55, 370–387.

Ciannelli, L., Brodeur, R.D., Swartzman, G.L., Salo, S., 2002. Physical and biological factors influencing the spatial distribution of age-0 walleye pollock (*Theragra chalcogramma*) around the Pribilof Islands, Bering Sea. Deep-Sea Res. II. 49, 6109-6126.

Coachman, L. K., 1986. Circulation, water masses, and fluxes on the southeastern Bering Sea shelf. Cont. Shelf Res., 5(1-2), 23-108. doi:10.1016/0278-4343(86)90011-7.

Crane, K., Ostrovskiy, A., 2015. Russian-American Long-term Census of the Arctic: RUSALCA. Oceanography. 1:28(3), 18-23.

Danielson, S.L., Ahkinga, O., Ashjian, C., Basyuk, E., Cooper, L.W., Eisner, L., Farley, E., Iken, K.B., Grebmeier, J.M., Juranek, L., Khen, G., Jayne, S., Kikuchi, T., Ladd, C., Lu, K., McCabe, Moore, G.W.K., Nishino, S., Ozenna, F., Pickart, R.S., Polyakov, I., Stabeno, P.J., Thoman, R., Williams, W.J., Wood, K., Weingartner, T.J., 2020. Manifestation and consequences of warming and altered heat fluxes over the Bering and Chukchi Sea continental shelves. Deep-Sea Res. II. https://doi.org/10.1016/j.dsr2.2020.104781.

Duffy-Anderson, J.T., Ciannelli, L., Honkalehto, T. Bailey, K.M., Sogard, S.M., Springer, A. and Buckley, T., 2003. Distribution of age-1 and age-2 walleye pollock in the Gulf of Alaska and Eastern Bering Sea: sources of variation and implications for higher trophic levels. Pp. 381-394. In: The Big Fish Bang: Proceedings from the 26th Annual Larval Fish Conference. Browman, H and A. Skiftesvik (eds.).

Duffy-Anderson, J.T., Stabeno, P., Andrews, A., Cieciel, K., Deary, A., Farley, E., Fugate, C., Harpold, C., Heintz, R., Kimmel, D., Kuletz, K., Lamb, J., Paquin, M., Porter, S., Rogers, L., Spear, A., Yasumiishi, E., 2019. Responses of the Northern Bering Sea and Southeastern Bering Sea pelagic ecosystems following record-breaking low winter sea ice. Geophys. Res. Lett. doi: 10.1029/2019GRL083396.

Duffy-Anderson, J.T., Stabeno, P.J., Siddon, E.C., Andrews, A.G., Cooper, D.W., Eisner, L.B., Farley, E.V., Harpold, C.E., Heintz, R.A., Kimmel, D.G., Sewall, F.F., Spear, A.H., and Yasumiishi, E., 2017. Return of warm conditions in the southeastern Bering Sea: phytoplankton-fish. PLOS One. https://doi.org/10.1371/journal.pone.0178955.

Eisner, L., Kivva, K., Baker, M., 2017. The role of the northern Bering Sea in modulating Arctic environments: Towards international interdisciplinary efforts. PICES Press, 25(1), 24-29.

Eisner, L., Napp, J., Mier, K., Pinchuk, A., Andrews A., 2014. Climate-mediated changes in zooplankton community structure for the eastern Bering Sea. Deep Sea Res II, 109: 157-171. doi: 10.1016/j.dsr2.2014.03.004.

Favorite, F., Dodimead, A.J., Nasu K., 1976. Oceanography of the Subarctic Pacific Region, 1960-71. International North Pacific Fisheries Commission Bull. 33, 187 p.

Fissel, B., Dalton, M., Garber-Yonts, B., Haynie, A., Kasperski, S., Lee, J., Lew, D., Lavoie, A., Seung, C., Sparks, K., Szymkowiak, M., Wise, S., 2019. Stock Assessment and Fishery Evaluation Report for the Groundfish Fisheries of the Gulf of Alaska and Bering Sea/Aleutian Island Area: Economic Status of the Groundfish Fisheries off Alaska, 2017, NPFMC, April, 2019. http://www.afsc.noaa.gov/refm/docs/2018/economic.pdf.

Haidvogel, D. B., Arango, H., Budgell, W. P., Cornuelle, B. D., Curchitser, E., Di Lorenzo, E., Fennel, K., Geyer, W. R., Hermann, A. J., Lanerolle, L., Levin, J., McWilliams, J. C., Miller, A. J., Moore, A. M., Powell, T. M., Shchep- etkin, A. F., Sherwood, C. R., Signell, R. P., Warner, J. C., and Wilkin, J., 2008. Ocean forecasting in terrain-following coor- dinates: Formulation and skill assessment of the Regional Ocean Modeling System, J. Comput. Phys., 227, 3595–3624, https://doi.org/10.1016/j.jcp.2007.06.016.

Haynie, A.C., Huntington, H.P., 2016. Strong connections, loose coupling: the influence of the Bering Sea ecosystem on commercial fisheries and subsistence harvests in Alaska. Ecol. Soc. 21(4): 6. doi:10.5751/ES-08729-210406.

Heintz, R. A., Siddon, E. C., Farley, Jr, E. V., and Napp, J. M., 2013. Climate-related changes in the nutritional condition of young-of-the-year walleye pollock (*Theragra chalcogramma*) from the eastern Bering Sea. Deep-Sea Res. II. 94, 150–156.

Hollowed, A.B., Wilson, C.D., Stabeno, P.J., Salo, S.A., 2007. Effect of ocean conditions on the cross-shelf distribution of walleye pollock (*Theragra chalcogramma*) and capelin (*Mallotus villosus*). Fish. Oceanogr. 16, 142–154. https://doi.org/10.1111/j.1365-2419.

Honkalehto, T., McCarthy, A., Ressler, P., and Jones, D., 2013. Results of the acoustic-trawl survey of walleye pollock (*Theragra chalcogramma*) on the U.S. and Russian Bering Sea Shelf in June–August 2012 (DY1207). AFSC Processed Rep. 2013-02. Alaska Fish. Sci. Cent., NOAA, Natl. Mar. Fish.Serv., 7600 Sand Point Way NE, Seattle WA 98115, USA.

Huntington, H.P., Danielson, S.L., Wiese, F.K., Baker, M., Boveng, P., Citta, J.J., De Robertis, A., Dickson, D.M.S., Farley, E., George, J.C., Iken, K., Kimmel, D.G., Kuletz, K., Levine, R., Quakenbush, L., Stabeno, P., Stafford, K.M., Stockwell, D., Wilson, C., 2020. Evidence suggests potential transformation of the Pacific Arctic ecosystem is underway. Nature Climate Change. https://doi.org/10.1038/s41558-020-0695-2.

Ianelli, J, Fissel, B., Holsman, K., Honktalehto, T., Kotwicki, S., Monnahan, C., Siddon, E., Stienessen, S., and Thorson, J., 2019. Chapter 1: Assessment of the walleye pollock stock in the Eastern Bering Sea. In: Stock assessment and fishery evaluation report for the groundfish resources of the Bering Sea/Aleutian Islands regions, Alaska Fisheries Science Center, National Marine Fisheries Service, Anchorage, Alaska, pp. 1–169.

Ianelli, J.N., Honkalehto, T., Barbeaux, S., Kotwicki, S., 2014. Chapter 1: Assessment of the walleye pollock stock in the Eastern Bering Sea. In Stock assessment and fishery evaluation report for the groundfish resources of the Bering Sea/Aleutian Islands regions, Alaska Fisheries Science Center, National Marine Fisheries Service, Anchorage, Alaska, pp. 55–156.

Kearney, K., Hermann, A., Cheng, W., Ortiz, I., Aydin, K., 2020. A coupled pelagic–benthic–sympagic biogeochemical model for the Bering Sea: documentation and validation of the BESTNPZ model (v2019.08.23) within a high-resolution regional ocean model. Geosci. Model Dev., 13, 597–650.

Khen, G.V., Basyuk, E.O., Vanin, N.S. Matveev, V.I., 2013. Hydrography and biological resources in the western Bering Sea. Deep-Sea Res. II. 94, 106-120.

Kimura, D.K., Kastelle, C.R., Goetz, B.J., Gburski, C.M., Buslov, A.V., 2006. Corroborating ages of walleye pollock (*Theragra chalcogramma*), Australian J. of Marine and Freshwater Research 57, 323-332.

Kinder, T.H., Schumacher, J.D., 1981. Circulation over the continental shelf of the Southeastern Bering Sea, in The Eastern Bering Sea Shelf: Oceanography and Resources, edited by D. W. Hood and J. A. Calder, pp. 53-75, University of Washington Press, Seattle, WA.

Kotwicki, S., Lauth R.R., 2013. Detecting temporal trends and environmentally-driven changes in the spatial distribution of groundfishes and crabs on the eastern Bering Sea shelf. Deep-Sea Res. II. 94, 231–243.

Kotwicki S., Buckley T., Honkaletho T., Walters G., 2005. Variation in the distribution of walleye pollock with temperature and implications for seasonal migration. Fish. Bull. 103, 574-587.

Kotwicki, S., Ianelli, J.N., Punt, A.E., 2014. Correcting density-dependent effects in abundance estimates from bottom trawl surveys. ICES J. Mar. Sci. 71, 1107-1116.

Kotwicki, S., Lauth, R.R., Williams, K., Goodman, S., 2017. Selectivity ratio a useful tool for comparing size selectivity of multiple survey gears. Fisheries Research. 191: 76-86.

Kotwicki, S., Ono, K., 2019. The effect of random and density dependent variation in sampling efficiency on variance of abundance estimates from fishery surveys. Fish and Fisheries. 20 (4), 760-774. doi:10.1111/faf.12375

Ladd, C., 2014. Seasonal and interannual variability of the Bering Slope Current. Deep-Sea Res. II. 109, 5-13.

Laurel, B., Copeman, L., Spencer, M., Iseri, P., 2018. Comparative effects of temperature on rates of development and survival of eggs and yolk-sac larvae of Arctic cod (*Boreogadus saida*) and walleye pollock (*Gadus chalcogrammus*). ICES J. Mar. Sci. 75(7), 2403-2412.

Laurel, B., Spencer, M., Iseri, P., Copeman, L., 2015. Temperature-dependent growth and behavior of juvenile Arctic cod (*Boreogadus saida*) and co-occurring North Pacific gadids. Polar Biology. 39(6), 1127-1135.

Lauth, R.R., 2011. Results of the 2010 eastern and northern Bering Sea continental shelf bottom trawl survey of groundfish and invertebrate fauna. United States Department of Commerce, NOAA Technical Memorandum. NMFS-AFSC-227. p. 256.

Lauth, R. R., Dawson, E.J., Conner, J., 2019. Results of the 2017 eastern and northern Bering Sea continental shelf bottom trawl survey of groundfish and invertebrate fauna. U.S. Dep. Commer., NOAA Tech. Memo. NMFS-AFSC-396, p. 260.

Locarnini, R.A., Mishonov, A.V., Antonov, J.I., Boyer, T.P., Garcia, H.E., Baranova, O.K., Zweng, M.M., Paver, C.R., Reagan, J.R., Johnson, D.R., Hamilton, M., Seidov, D., 2013. World Ocean Atlas 2013, vol. 1: Temperature, in: S. Levitus (Ed.). NOAA Atlas NESDIS, 73, 40 p.

Luchin, V.A., Menovshchikov, V.A., 1999. Chapter 7: Non-periodic currents. In Hydrometeorology and hydrochemistry of the seas/ Volume10: Bering Sea, Part 1, Gidrometeoizdat, Sankt-Peterburg, pp. 193-219.

McLean, M., Mouillot, D., Auber, A. 2018. Ecological and life history traits explain a climate-induced shift in a temperate marine fish community. Mar. Ecol. Prog. Ser. 606, 175-186.

Meier, W.N., Fetterer, F., Savoie, M., Mallory, S., Duerr, R., Stroeve, J., 2017. NOAA/NSIDC Climate Data Record of Passive Microwave Sea Ice Concentration, Version 3, Boulder, Colorado USA, National Snow and Ice Data Center. doi: https://doi.org/10.7265/N59P2ZTG.

Mueter, F.J., Litzow, M.A., 2008. Sea ice alters the biogeography of the Bering Sea continental shelf. Ecol. Appl. 18(2), 309 – 320.

Olla, B.L., Davis, M.W., 1990. Behavioral responses of juvenile walleye pollock (*Theragra chalcogramma* Palls) to light, thermoclines, and food: possible role in vertical distribution. J. Exp. Mar. Biol. Ecol. 135, 59-68.

O'Leary, C.A., Kotwicki, S., Hoff, G.R., Thorson, J.T., Kulik, V.V., Ianelli, J.N., Lauth, R.R., Nichol, D.G., Conner, J., Punt, A.E. *In Review.* Estimating spatiotemporal availability of Bering Sea groundfish species to fishery-independent surveys using area-swept biomass indices from multiple surveys.

Orlov, A.M., Benzik, A.N., Vedishcheva, E.V., Gafitsk, S.V., Gorbatenko, K.M., Goryanina, S.V., Zubarevich, V.L., Kodryan, K.V., Nosov, M.A., Orlova, S.Yu., Pedchenko, A.P.,Rybakov, M.O., Sokolov, A.M., Somov, A.A., Subbotin, S.N., Taptygin, M.Yu., Firsov, Yu.L., Khleborodov, A.S., Chikilev, V.G., 2020. Fisheries research in the Chukchi Sea at the *RV Professor Levanidov* in August 2019: some preliminary results. Trudy VNIRO. Vol. 178. P. 206–220. DOI: 10.36038/2307-3497-2019-178-206-220.

Overland, J.E., Stabeno, P., Ladd, C., Wang, M., Bond, N., 2019. Eastern Bering Sea Climate - FOCI, in: Siddon, E., Zador, S. (Eds.), Ecosystem Status Report 2019: Eastern Bering Sea. NOAA Fisheries.

Panteleev, G., Yaremchuk, M., Stabeno, P.J., Luchin, V., Nechaev, D.A., Kikuchi, T., 2011. Dynamic topography of the Bering Sea. J. Geophys. Res. - Oceans 116.

Peng, G., Meier, W.N., Scott, D., Savoie, M., 2013. A long-term and reproducible passive microwave sea ice concentration data record for climate studies and monitoring, Earth Syst. Sci. Data. 5, 311-318. https://doi.org/10.5194/essd-5-311-2013.

Petrik, C.M., Duffy-Anderson, J.T., Castruccio, F., Curchitser, E.N., Danielson, S.L., Hedstrom, K., Mueter, F., 2016. Modelled connectivity between walleye pollock (*Gadus chalcogrammus*) spawning and age-0 nursery areas in warm and cold years with implications for juvenile survival. ICES J. Mar. Sci. 73(7), 1890-1900.

Saha, S., Moorthi, S., Pan, H. L., Wu, X., Wang, J., Nadiga, S., Tripp, P., Kistler, R., Woollen, J., Behringer, D., Liu, H., Stokes, D., Grumbine, R., Gayno, G., Wang, J., Hou, Y. T., Chuang, H. Y., Juang, H. M. H., Sela, J., Iredell, M., Treadon, R., Kleist, D., Van Delst, P., Keyser, D., Derber, J., Ek, M., Meng, J., Wei, H., Yang, R., Lord, S., Van Den Dool, H., Kumar, A., Wang, W., Long, C., Chelliah, M., Xue, Y., Huang, B., Schemm, J. K., Ebisuzaki, W., Lin, R., Xie, P., Chen, M., Zhou, S., Higgins, W., Zou, C. Z., Liu, Q., Chen, Y., Han, Y., Cucurull, L., Reynolds, R. W., Rutledge, G., and Goldberg, M., 2010. The NCEP climate forecast system reanalysis, B. Am. Meteorol. Soc., 91, 1015–1057, https://doi.org/10.1175/2010BAMS3001.1.

Savin, A.B., 2011. Methodical recommendations on planning and conducting bottom trawl surveys in the Far Eastern basin, Issled. Vodn. Biol. Resur. Kamchatki i Sev.-Zap. Chasti Tikhogo Okeana (Studies of water biological resources in Kamchatka and North-West Pacific) 22, 68–78.

Savin, A.B., 2018. Fish resources in near-bottom biotopes of the shelf and the upper edge of the continental slope in the northwestern Bering Sea. Russian Journal of Marine Biology. 44(7), 1–18. ISSN 1063-0740. Original Russian Text © A.B. Savin, 2018, published in Izvestia TINRO.

Schabetsberger, R., Sztatecsny, M., Drozdowski, G., Brodeur, R.D., Swartzman, G.L., Wilson, M.T., Winter, A.G., Napp, J.M., 2003. Size-dependent, spatial, and temporal variability of juvenile walleye pollock (*Theragra chalcogramma*) feeding at a structural front in the southeast Bering Sea. Mar. Ecol. 24, 141-164.

Smart, T., Duffy-Anderson, J.T., Horne, J., 2012. Alternating climate states influence walleye pollock life stages in the southeastern Bering Sea. Mar. Ecol. Prog. Ser. 455, 257-267.

Smith, R.L., Paul, A.J., Paul, J.M., 1988. Aspects of energetics of adult walleye pollock, *Theragra chalcogramma* (Pallas), from Alaska. J. Fish Biol. 33, 445-454.

Spies, I., Gruenthal, K.M., Drinan, D.P., Hollowed, A., Stevenson, D.E., Tarpey, C.M., Hauser, L., 2019. Genetic evidence of a northward range expansion in the eastern Bering Sea stock of Pacific cod. Evolutionary Applications. https://doi.org/10.1111/eva.12874

Stabeno, P.J., Bell, S.W., 2019. Extreme conditions in the Bering Sea (2017–2018): Record-breaking low sea-ice extent. Geophysical Research Letters, 46, 8952–8959. https://doi.org/10.1029/2019GL083816

Stabeno, P.J., Danielson, S., Kachel, D., Kachel, N.B., Mordy, C.W., 2016. Currents and transport on the eastern Bering Sea shelf: An integration of over 20 years of data. Deep-Sea Res. II. 134, 13–29. https://doi.org/10.1016/j.dsr2.2016.05.010

Stabeno, P.J., Reed, R.K., 1994. Circulation in the Bering Sea basin observed by satellite-tracked drifters: 1986-1993. J. Phys. Oceanogr. 24, 848-854.

Stauffer, G., 2004. NOAA protocols for groundfish bottom-trawl surveys of the Nation's fishery resources. United States Department of Commerce. NOAA Technical Memorandum. NMFS-F/SPO-65. p. 205.

Stepanenko, M.A., Gritsay, E.V., 2016. Assessment of stock, spatial distribution, and recruitment of walleye pollock in the northern and eastern Bering Sea. Izvestia TINRO (Newsletters of Pacific Fish. Res. Center), 185, 16-30.

Stevenson, D.E., Lauth, R.R., 2019. Bottom trawl surveys in the northern Bering Sea indicate recent shifts in the distribution of marine species. Polar Biol. 42, 407–421. https://doi.org/10.1007/s00300-018-2431-1.

Sturdevant, M.V., Brase, A.L.J., Hulbert, L.B., 2001. Feeding habits, prey fields, and potential competition of young-of-the-year walleye pollock (*Theragra chalcogramma*) and Pacific herring (*Clupea pallasi*) in Prince William Sounds, Alaska, 1994-1995. Fish. Bull. 99, 482-501.

Thorson, J.T., Ianelli, J.N., Kotwicki, S., 2017. The relative influence of temperature and size-structure on fish distribution shifts: A case-study on walleye pollock in the Bering Sea. Fish and Fisheries 18(6), 1073-1084.

Vestfals, C., Ciannelli, L., Hoff, G., 2016. Changes in habitat utilization of slope-spawning flatfish across a bathymetric gradient. ICES J. Mar. Sci. 73(7), 1875-1889.

Wakabayashi, K., Bakkala, R.G., Alton, M.S., 1985. Methods of the U.S.-Japan demersal trawl surveys, p. 7-29. In: R.G. Bakkala and K. Wakabayashi (editors), Results of cooperative U.S.-Japan groundfish investigations in the Bering Sea during May-August 1979. Int. North Pac. Fish. Comm. Bull. 44.

Woodgate, R.A., Aagaard, K., 2005. Revising the Bering Strait freshwater flux into the Arctic Ocean, Geophys. Res. Lett., 32(2), https://doi.org/10.1029/2004GL021747.

Wyllie-Echeverria, T., Wooster, W.S., 1998. Year-to-year variations in Bering Sea ice cover and some consequences for fish distributions. Fish. Oceanogr. 7, 159-170.

Zuenko, Y.I., Basyuk, E.O., 2017. Changing oceanographic conditions influence on species composition and abundance of zooplankton on the fishing grounds at Cape Navarin and their importance for the Russian pollock fishery in the Bering Sea. Izvestia TINRO (Newsletters of Pacific Fish. Res. Center). 189, 103-120.

Table 1. Survey timing and mean surface and bottom temperatures (T, °C) for surveys on the SE, NE and NW shelves. See Fig. 7 for differences in areas surveyed among years (e.g., no sampling in Anadyr Bay (NW) in 2019 or Norton Sound (NE) in 2018).

Year	SE	NE	NW
2010	June 3 – August 4	July 23 – August 15	July 10 – September 6
Surface T	5.34	9.35	9.00
Bottom T	1.42	2.01	1.97
2017	June 3 – July 31	August 1 – August 26	June 7 – July 30
Surface T	7.99	9.63	9.08
Bottom T	2.67	4.37	2.46
2018	June 3 – July 30	July 31 – August 14	July 31 – August 18 (midwater trawl)
Surface T	7.59	10.23	9.80
Bottom T	4.14	3.94	2.94
2019	June 3 – July 28	July 29 – August 20	July 26 – August 8
Surface T	9.24	10.85	9.69
Bottom T	4.34	5.75	2.44

Table 2. Mean proportions of pollock abundance (% of total weight) for a) adult (> age-2) and b) age-1 pollock, and c) number of successful tows by bottom temperature (°C) and bottom depth (nearest 20 m) for US groundfish bottom trawl surveys (SE and NE), 1987-2019. NA indicates the number of tows = 0. Top 95% of non-zero values are in bold. Darker shading indicates higher values.

a)

Bottom	**Mean Bottom Temperature**																	
Depth	**-2**	**-1**	**0**	**1**	**2**	**3**	**4**	**5**	**6**	**7**	**8**	**9**	**10**	**11**	**12**	**13**	**14**	**15**
20	NA	0	0	0	0	0	0.001	0.001	0.001	0	0	0	0	0	0	0	0	0
40	0	0.001	0.003	**0.005**	**0.006**	**0.008**	**0.006**	0.003	0.001	0.001	0.001	0	0	0	0	NA	NA	NA
60	0	0.004	**0.009**	**0.015**	**0.022**	**0.038**	**0.028**	**0.019**	**0.005**	0	NA	NA	NA	NA	NA	NA	NA	NA
80	0.002	**0.008**	**0.015**	**0.029**	**0.029**	**0.032**	**0.043**	**0.046**	**0.014**	NA	NA	NA	NA	NA	NA	NA	NA	NA
100	0.002	**0.008**	**0.020**	**0.058**	**0.045**	**0.044**	**0.028**	**0.018**	0.001	0	NA	NA	NA	NA	NA	NA	NA	NA
120	0	0	**0.014**	**0.021**	**0.039**	**0.045**	**0.030**	**0.015**	0	NA	NA	NA	NA	NA	NA	NA	NA	NA
140	NA	NA	0.002	**0.014**	**0.029**	**0.034**	**0.014**	0.001	NA	0	NA	NA	NA	NA	NA	NA	NA	NA
160	NA	NA	0.001	**0.011**	**0.022**	**0.035**	**0.011**	0	0	NA	NA	NA	NA	NA	NA	NA	NA	NA
180	NA	NA	NA	NA	**0.017**	**0.023**	0	NA	NA	NA	NA	NA	NA	NA	NA	NA	NA	NA
200	NA	NA	NA	NA	NA	0.001	0.001	NA	NA	NA	NA	NA	NA	NA	NA	NA	NA	NA
Sum	**0.004**	**0.021**	**0.064**	**0.153**	**0.209**	**0.260**	**0.162**	**0.103**	**0.022**	**0.001**	**0.001**	**0**	**0**	**0**	**0**	**0**	**0**	**0**

b)

Bottom	**Mean Bottom Temperature**																	
Depth	**-2**	**-1**	**0**	**1**	**2**	**3**	**4**	**5**	**6**	**7**	**8**	**9**	**10**	**11**	**12**	**13**	**14**	**15**
20	NA	0	0	0	0.003	0.004	**0.006**	**0.005**	**0.010**	**0.005**	0.002	0.002	**0.006**	0.002	0.001	0	0	0
40	0	0.004	**0.008**	**0.008**	**0.010**	**0.017**	**0.012**	**0.007**	**0.006**	**0.010**	0.002	0.004	0.002	0.004	0.004	NA	NA	NA
60	0.002	**0.006**	**0.015**	**0.018**	**0.020**	**0.017**	**0.014**	**0.009**	**0.006**	0.001	NA	NA	NA	NA	NA	NA	NA	NA
80	**0.007**	**0.014**	**0.022**	**0.022**	**0.028**	**0.034**	**0.014**	**0.005**	0	NA	NA	NA	NA	NA	NA	NA	NA	NA
100	0.002	**0.021**	**0.041**	**0.050**	**0.092**	**0.054**	**0.014**	0.001	0	0	NA	NA	NA	NA	NA	NA	NA	NA
120	0	0.001	**0.015**	**0.047**	**0.058**	**0.042**	**0.010**	0.001	0	NA	NA	NA	NA	NA	NA	NA	NA	NA
140	NA	NA	**0.005**	**0.026**	**0.053**	**0.032**	0.004	0	NA	0	NA	NA	NA	NA	NA	NA	NA	NA
160	NA	NA	0.001	**0.009**	**0.011**	0.004	0.003	0	0	NA	NA	NA	NA	NA	NA	NA	NA	NA
180	NA	NA	NA	NA	0	0.004	0	NA	NA	NA	NA	NA	NA	NA	NA	NA	NA	NA
200	NA	NA	NA	NA	NA	0	0	NA	NA	NA	NA	NA	NA	NA	NA	NA	NA	NA
Sum	**0.011**	**0.046**	**0.107**	**0.18**	**0.275**	**0.208**	**0.077**	**0.028**	**0.022**	**0.016**	**0.004**	**0.006**	**0.008**	**0.006**	**0.005**	**0**	**0**	**0**

c)

Bottom	**Mean Bottom Temperature**																	
Depth	**-2**	**-1**	**0**	**1**	**2**	**3**	**4**	**5**	**6**	**7**	**8**	**9**	**10**	**11**	**12**	**13**	**14**	**15**
20	0	0	5	14	16	53	141	103	146	79	56	26	46	29	30	19	8	1
40	2	77	90	133	390	416	489	285	174	65	29	8	5	5	2	0	0	0
60	137	360	374	388	496	396	366	147	62	6	0	0	0	0	0	0	0	0
80	170	346	377	341	473	433	377	109	26	0	0	0	0	0	0	0	0	0

100	21	84	178	249	410	364	294	64	4	0	0	0	0	0	0	0	0	0
120	0	2	32	125	273	319	444	74	1	0	0	0	0	0	0	0	0	0
140	0	0	15	86	319	265	352	32	0	0	0	0	0	0	0	0	0	0
160	0	0	2	12	35	60	118	3	1	0	0	0	0	0	0	0	0	0
180	0	0	0	0	10	16	9	0	0	0	0	0	0	0	0	0	0	0
200	0	0	0	0	0	2	6	0	0	0	0	0	0	0	0	0	0	0

Gray scale for a) and b)	Gray scale for c)
0	0
0.001 - 0.004	1 - 49
0.005 - 0.009	50 - 99
0.010 - 0.019	100 - 199
0.020 - 0.029	200 - 299
0.030 - 0.039	300 - 399
> = 0.040	> = 400

Figure captions

Fig. 1. Study Area. Regions sampled include the northwest (NW) shelf in the Russian EEZ, and the northeast (NE) and southeast (SE) shelf in the US EEZ of the Bering Sea. Contours denote the 50 m, 100 m, and 200 m isobaths.

Fig. 1 insert. Map of currents in the eastern Bering Sea. ACC = Alaska Coastal Current, ANSC = Aleutian North Slope Current, BSC = Bering Slope Current, EKC = East Kamchatka Current, and NC = Navarin Current.

Fig. 2. Maximum sea-ice extent (defined as 30% concentration) in the Bering Sea for 2010, 2017, 2018, 2019.

Fig. 3. Ice retreat day of year: the date when sea-ice concentration fell below 30% and remained below 30% for the remainder of the summer.

Fig. 4. Bottom temperatures from summer fisheries oceanography surveys for 2010, 2017, 2018, and 2019, normalized to July 15. The cold pool (< 2°C) is designated by blue with the 0°C contour designated by the bold line.

Fig. 5. Bottom currents averaged over March, April and May for 2010, 2017, 2018, and 2019 from the Bering10K model.

Fig. 6. Bottom currents averaged over June, July and August for 2010, 2017, 2018, and 2019 from the Bering10K model.

Fig. 7. Adult biomass distribution (kg km^{-2}) for pollock on the Bering Sea shelf from bottom trawls and pelagic (midwater) trawls (2018, NW area) in relatively cold conditions of 2010, and warm conditions of 2017, 2018, and 2019 during summer. See Table 1 for surveys dates by region and year. Fisheries sampling stations indicated by dots. US-Russia transboundary shown by dashed line.

Fig. 8. Pollock distribution in the NW Bering Sea in August 2018 from the acoustic survey. Color bar indicates metric ton/nautical mile^2. The data are kindly presented by Dr. M.Y. Kuznetsov, TINRO.

Fig. 9. Age-1 (juvenile) pollock abundance (number km^{-2}) for 2010, 2017, 2018, and 2019 from trawl surveys as described in Fig.7.

Fig. 10. Size structure of pollock in Russian region (NW) and in US regions (NE, SE). Regions are shown in Figure 1. Note scale change for NE in 2010. Frequency are % of total individuals. Length data not shown for the NW in 2018 (midwater trawl data).

Appendix A:

Fig. A.1. Histograms of pollock lengths at age-3 and age-4 from US surveys. Frequency indicates number of individuals.

Fig. A.2. Oceanography stations for the US and Russian surveys in 2010, 2017, 2018, and 2019. The isobaths 50, 100, and 250 m are shown by thin lines, and the Russian EEZ border by a dotted line.

Fig. A.3. Adult pollock biomass (kg/ha) for 2010, 2017, 2018, and 2019 from US NOAA eastern Bering Sea bottom trawl surveys. Bottom temperature < 0 °C shown by blue contour and ≥ 6°C by red contour.

Fig. A.4. Age-1 pollock biomass (kg/ha) for 2010, 2017, 2018, and 2019 from US NOAA eastern Bering Sea bottom trawl surveys. Bottom temperature < 0 °C shown by blue contour and ≥ 6°C by red contour.

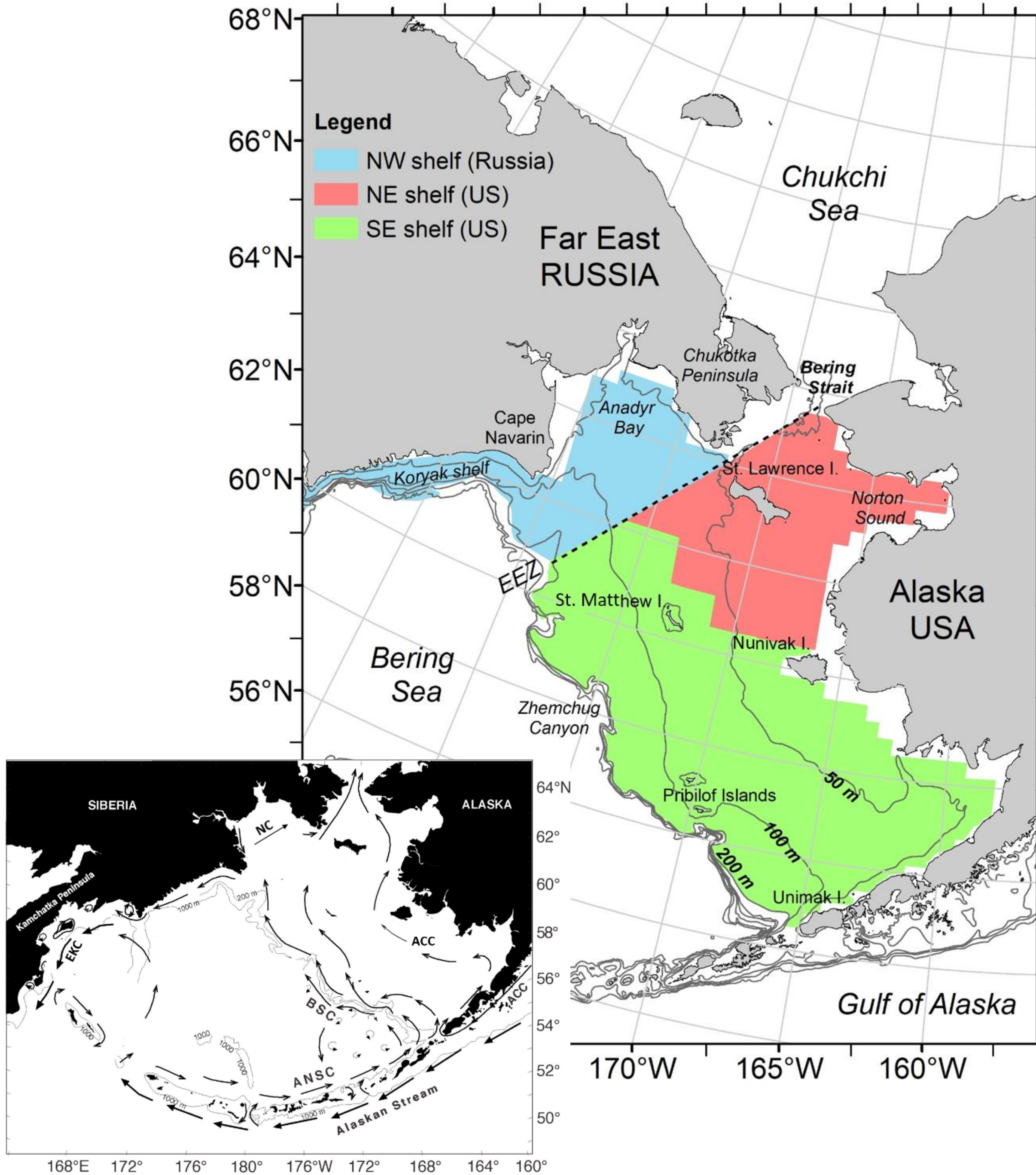

68°N
66°N
64°N
62°N
60°N
58°N
56°N
Legend
NW shelf (Russia)
NE shelf (US)
SE shelf (US)
Far East RUSSIA
Chukchi Sea
Chukotka Peninsula
Bering Strait
Cape Navarin
Anadyr Bay
Koryak shelf
St. Lawrence I.
Norton Sound
EEZ
St. Matthew I.
Alaska USA
Nunivak I.
Bering Sea
Zhemchug Canyon
Pribilof Islands
50 m
100 m
200 m
Unimak I.
Gulf of Alaska
170°W
165°W
160°W
SIBERIA
ALASKA
Kamchatka Peninsula
NC
EKC
ACC
BSC
ANSC
Alaskan Stream
1000 m
200 m
64°N
62°
60°
58°
56°
54°
52°
50°
168°E
172°
176°
180°
176°W
172°
168°
164°
160°

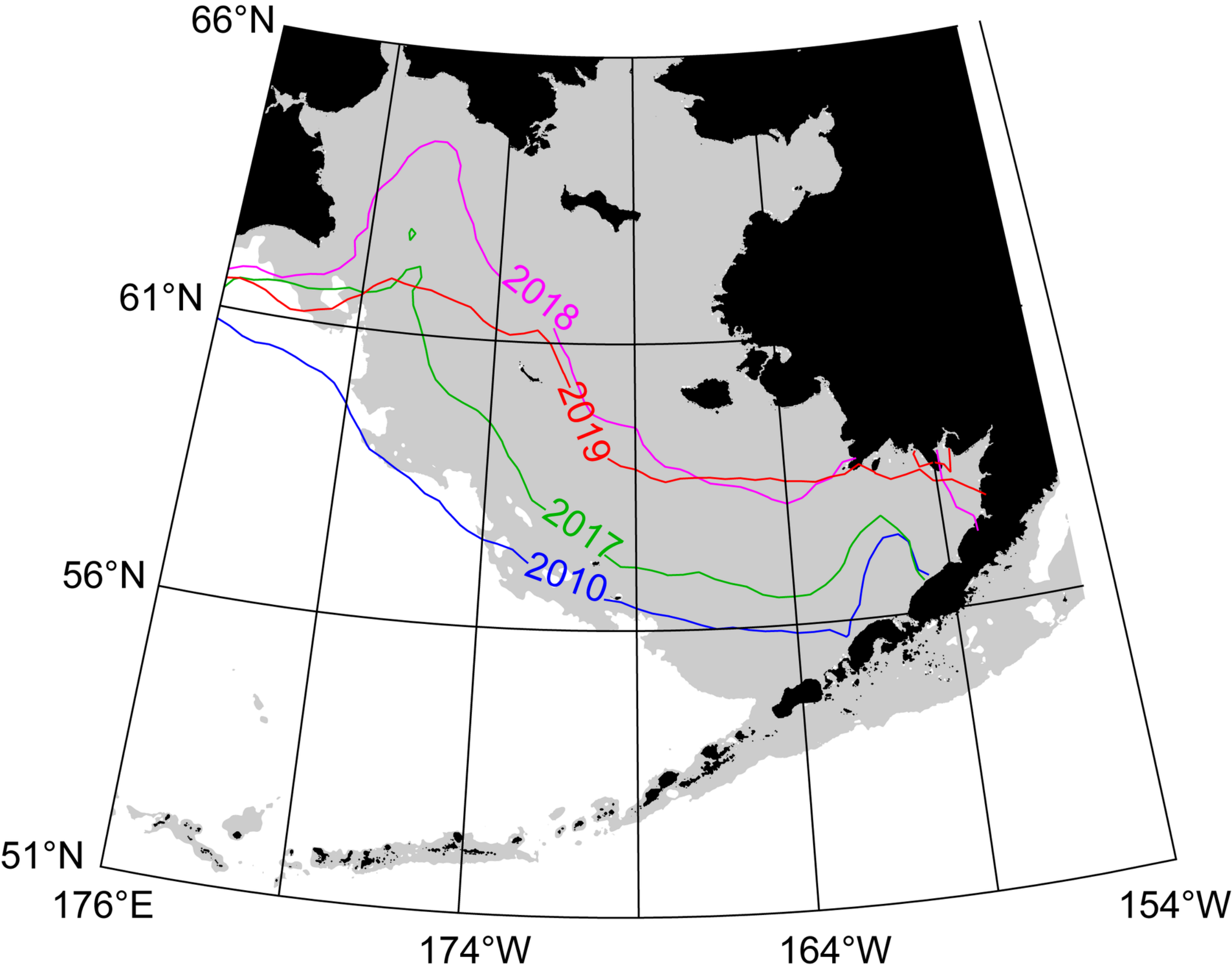
66°N
61°N
56°N
51°N
176°E
174°W
164°W
154°W
2018
2019
2017
2010

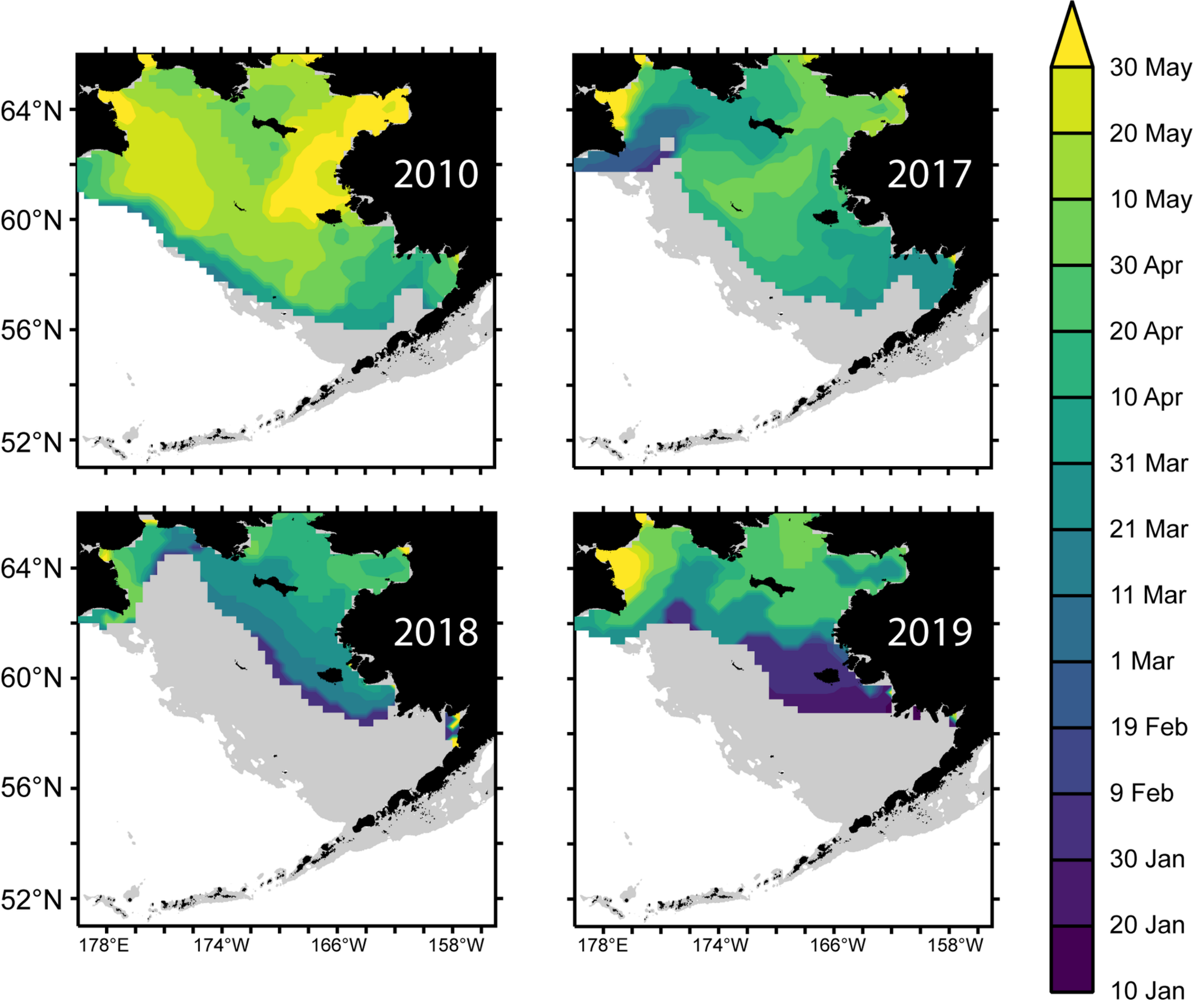

2010
2017
2018
2019
64°N
60°N
56°N
52°N
178°E
174°W
166°W
158°W
30 May
20 May
10 May
30 Apr
20 Apr
10 Apr
31 Mar
21 Mar
11 Mar
1 Mar
19 Feb
9 Feb
30 Jan
20 Jan
10 Jan

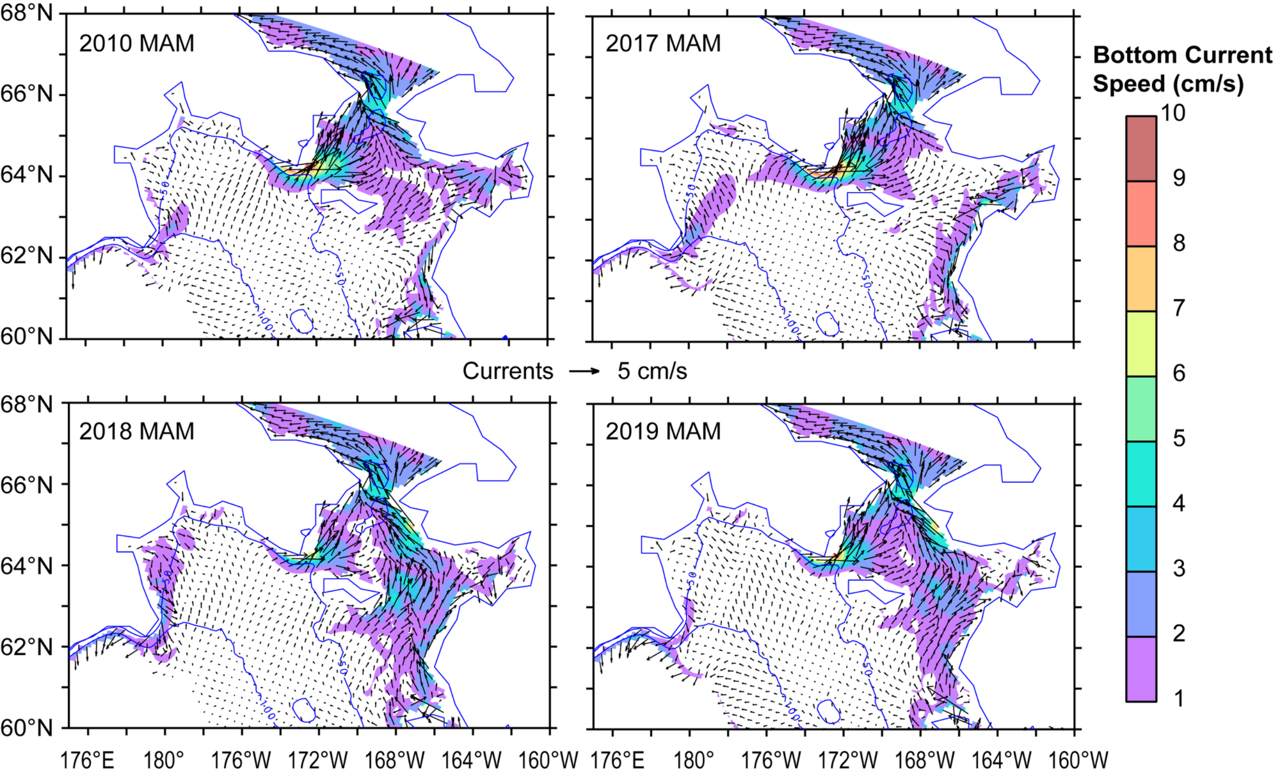

2010 MAM
2017 MAM
2018 MAM
2019 MAM
Bottom Current Speed (cm/s)
10
9
8
7
6
5
4
3
2
1
Currents
5 cm/s
68°N
66°N
64°N
62°N
60°N
176°E
180°
176°W
172°W
168°W
164°W
160°W
50
100

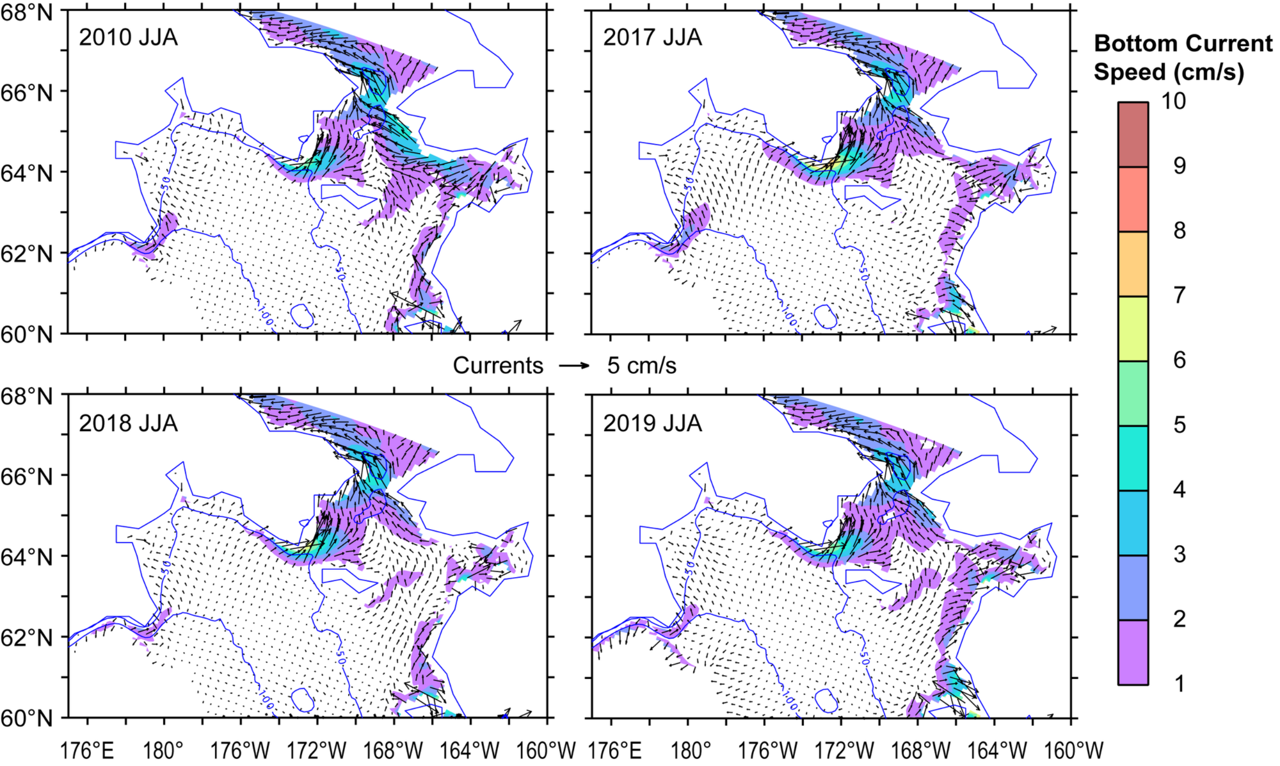

2010 JJA
2017 JJA
2018 JJA
2019 JJA
Bottom Current Speed (cm/s)
10
9
8
7
6
5
4
3
2
1
Currents
5 cm/s
68°N
66°N
64°N
62°N
60°N
176°E
180°
176°W
172°W
168°W
164°W
160°W
50
100

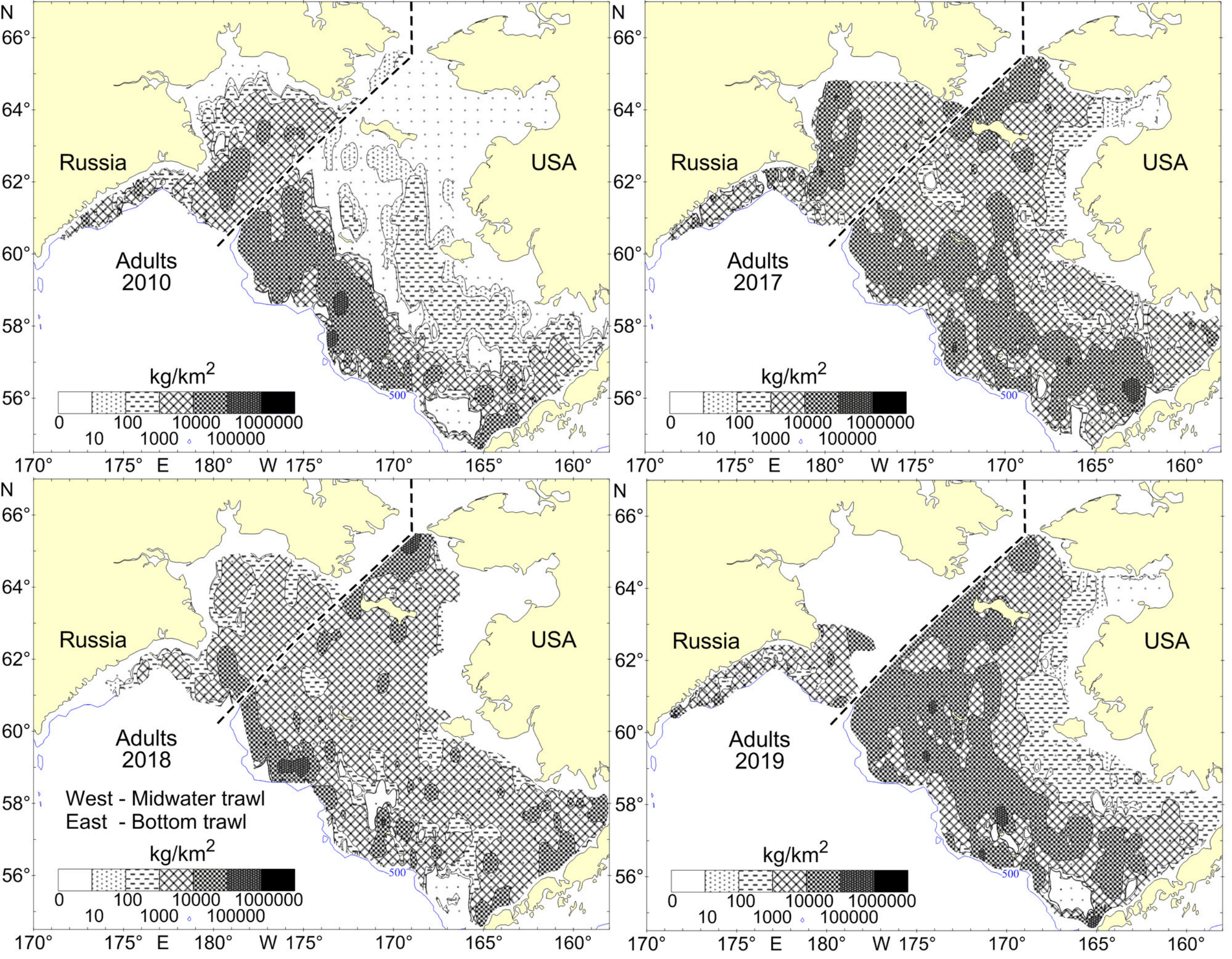
N
66°
64°
62°
60°
58°
56°
Russia
USA
Adults
2010
500
kg/km2
0
10
100
1000
10000
100000
1000000
170°
175°
E
180°
W
175°
170°
165°
160°
Adults
2017
Adults
2018
West - Midwater trawl
East - Bottom trawl
Adults
2019

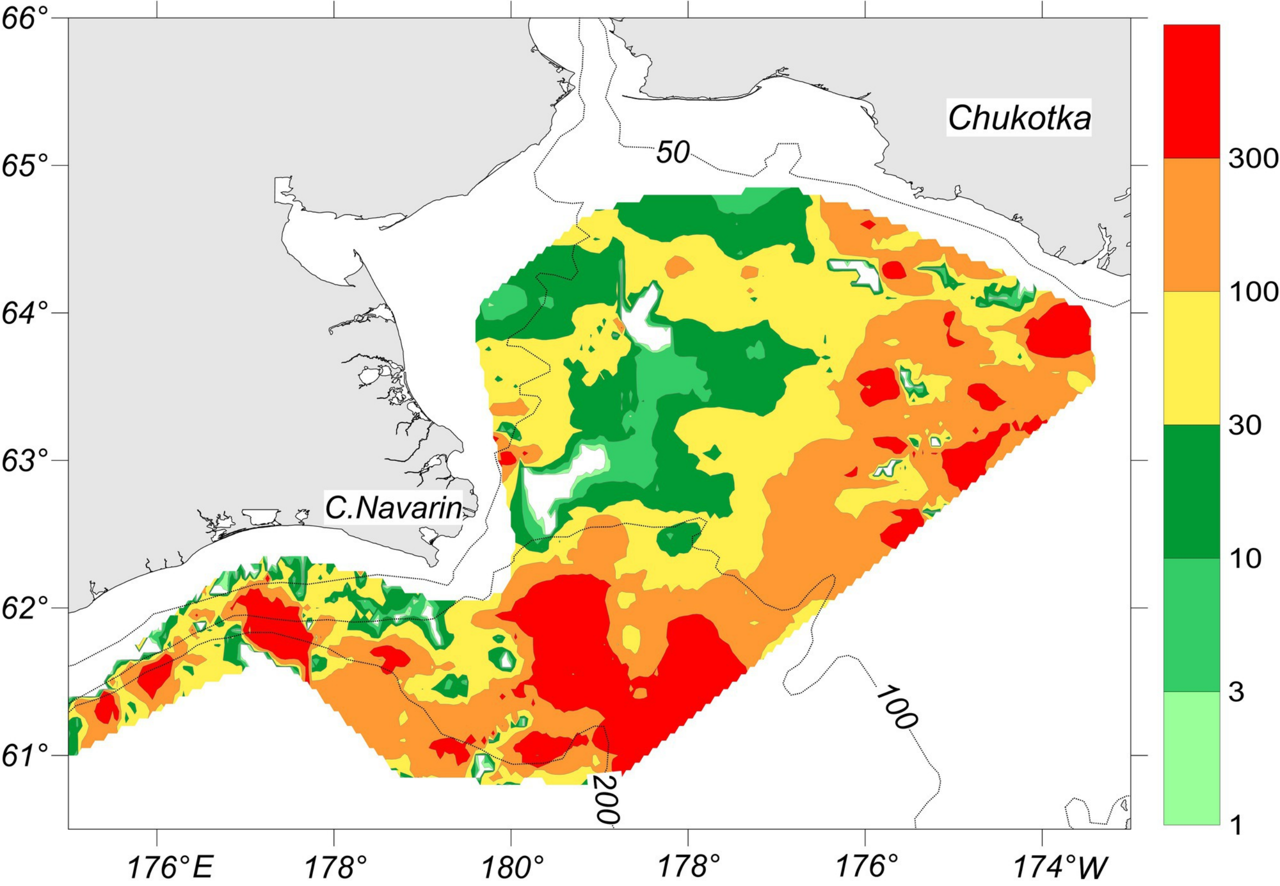

66°
65°
64°
63°
62°
61°
176°E
178°
180°
178°
176°
174°W
Chukotka
C.Navarin
50
100
200
300
100
30
10
3
1

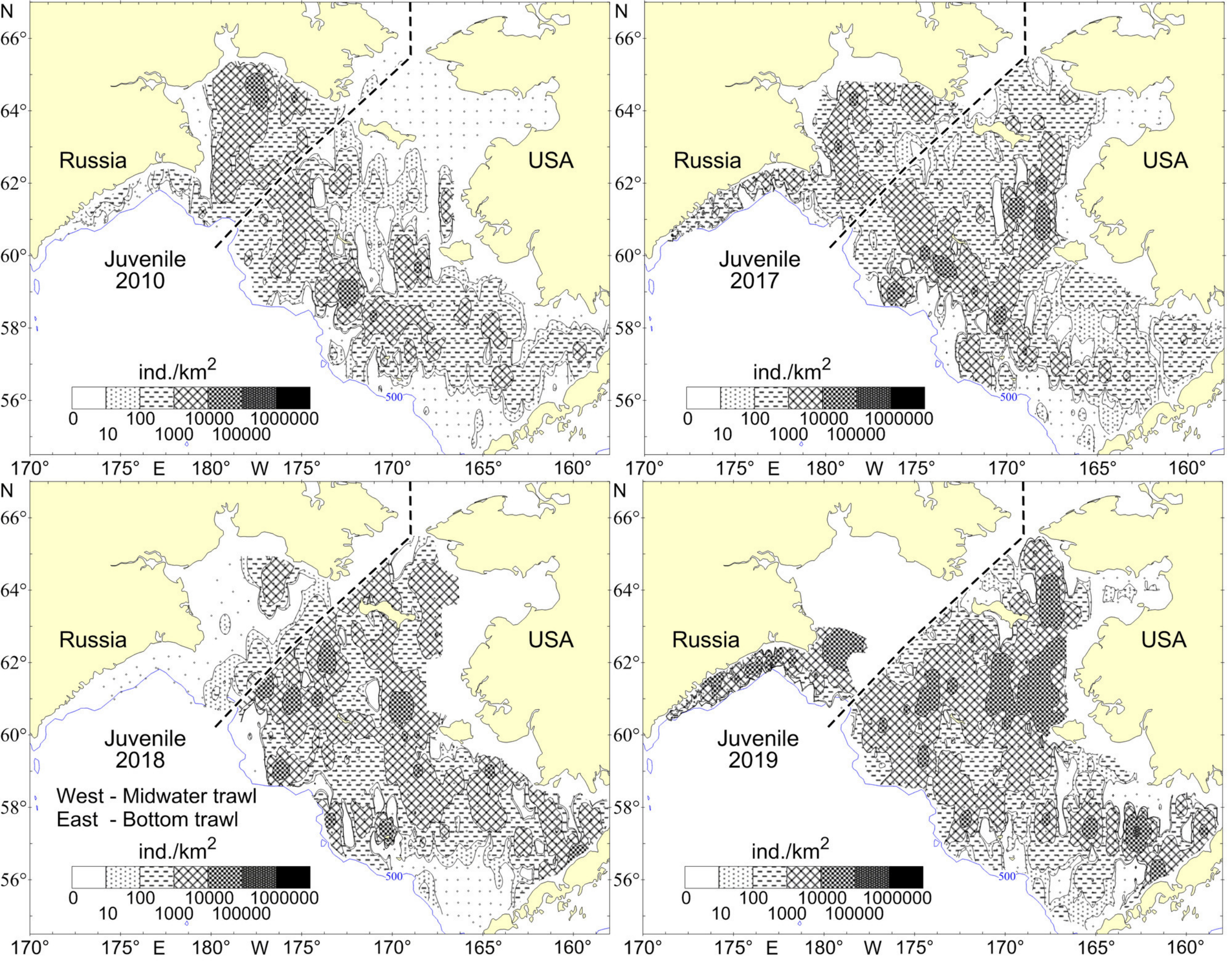

Russia
USA
Juvenile 2010
Juvenile 2017
Juvenile 2018
Juvenile 2019
West - Midwater trawl
East - Bottom trawl
ind./km2
0
10
100
1000
10000
100000
1000000
500
N
66°
64°
62°
60°
58°
56°
170°
175°
E
180°
W
175°
170°
165°
160°

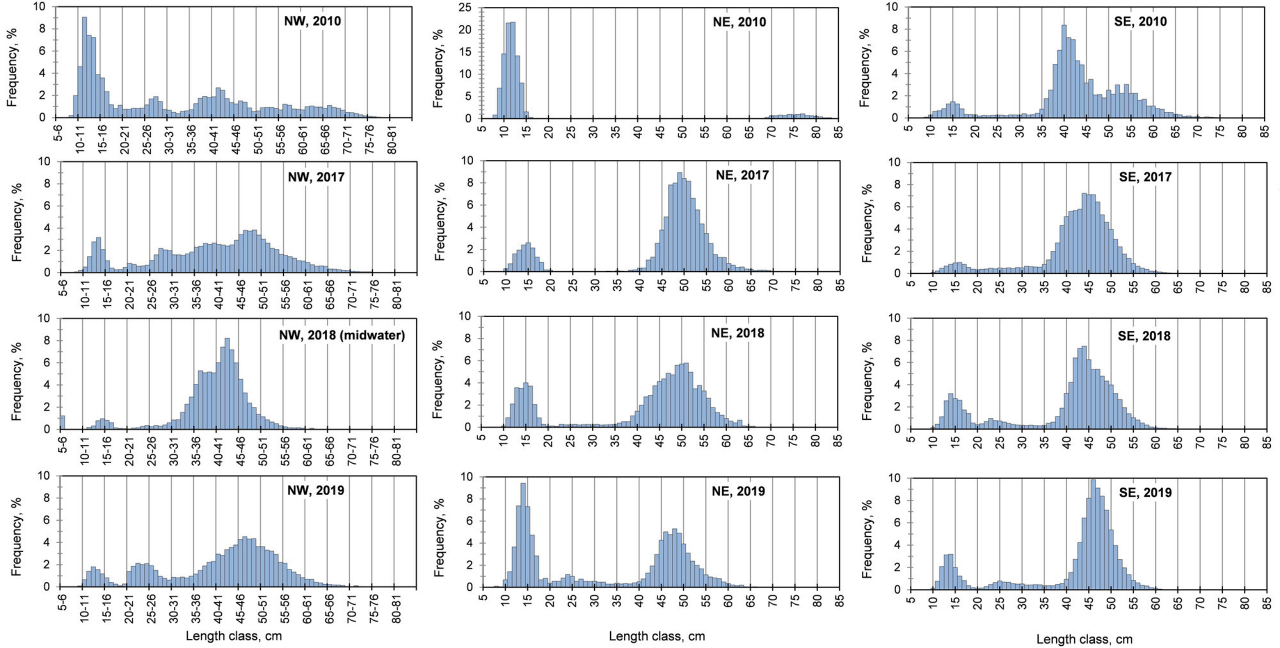
NW, 2010
NE, 2010
SE, 2010
NW, 2017
NE, 2017
SE, 2017
NW, 2018 (midwater)
NE, 2018
SE, 2018
NW, 2019
NE, 2019
SE, 2019
Frequency, %
Length class, cm